AD-787 617

DEVELOPMENT OF A LOW-DENSITY AMMO-
NIUM NITRATE/FUEL OIL EXPLOSIVE AND
MODELING OF ITS DETONATION PROPERTIES

M. W. McKay, et al

Physics International Company

REPORT DOCUMENTATION PAGE	READ INSTRUCTIONS BEFORE COMPLETING FORM

1. REPORT NUMBER	2. GOVT ACCESSION NO.	3. RECIPIENT'S CATALOG NUMBER
DNA 3351 F		AD-787617

4. TITLE (and Subtitle)	5. TYPE OF REPORT & PERIOD COVERED
DEVELOPMENT OF A LOW-DENSITY AMMONIUM NITRATE/FUEL OIL EXPLOSIVE AND MODELING OF ITS DETONATION PROPERTIES	Final Report-25 Oct.71- 30 Dec. 72
	6. PERFORMING ORG. REPORT NUMBER PIFR-383-Vol. II

7. AUTHOR(s)	8. CONTRACT OR GRANT NUMBER(s)
M.W. McKay, S.L. Hancock, and D. Randall	DNA001-72-C-0052

9. PERFORMING ORGANIZATION NAME AND ADDRESS	10. PROGRAM ELEMENT, PROJECT, TASK AREA & WORK UNIT NUMBERS
Physics International Company 2700 Merced Street San Leandro, California 94577	NWET L17CAXS, X301,01/02/03

11. CONTROLLING OFFICE NAME AND ADDRESS	12. REPORT DATE
Director Defense Nuclear Agency Washington D.C. 20305	October 1974
	13. NUMBER OF PAGES 62

14. MONITORING AGENCY NAME & ADDRESS(If different from Controlling Office)	15. SECURITY CLASS. (of this report)
	Unclassified
	15a. DECLASSIFICATION/DOWNGRADING SCHEDULE

16. DISTRIBUTION STATEMENT (of this Report)

Approved for public release; distribution unlimited

17. DISTRIBUTION STATEMENT (of the abstract entered in Block 20, if different from Report)

18. SUPPLEMENTARY NOTES

19. KEY WORDS (Continue on reverse side if necessary and identify by block number)

MINE THROW II Event   ANFO detonation properties
CACTUS Event
High explosives simulation
Ammonium nitrate/fuel oil explosive (ANFO)
Low density ANFO

20. ABSTRACT (Continue on reverse side if necessary and identify by block number)

A low-density ammonium nitrate/fuel oil (ANFO) explosive was developed by diluting the normal density explosive with low-density polystyrene beads. Stable detonations were achieved in mixtures having densities over the range 0.5 to 0.9 gm/cm^3. The detonation velocity was found to decrease approximately linearly with decreasing density. The explosive was found to have a long reaction time and required large charges with propagation distances on the

DD FORM 1473   EDITION OF 1 NOV 69 IS OBSOLETE

DNA 3351 F (Abstract) (cont.)

- order of 100 to 150 cm to establish a steady-state detona-
tion. The buildup of the detonation wave to its steady-
state velocity was successfully modeled using a grain-
burning reaction rate theory with a reaction time constant
of 100 μsec. A mixture having a density of 0.75 gm/cm^3 was
selected as the explosive for the MINE THROW II Event and
a mathematical model of its detonation properties was de-
veloped for use in the charge design calculations.

CONTENTS

1

ILLUSTRATIONS

Preceding page blank

ILLUSTRATIONS   (cont.)

SECTION 1
INTRODUCTION

Data from the MINE THROW I Event indicate that the detonation velocity and pressure for normal-density ANFO are considerably higher than was expected from values published in the literature. Pressures were measured on the order of 90 to 100 kbar, which is consistent with predictions made using an empirical technique (References 1 through 4) discussed later in this report. This has important consequences for the design of the MINE THROW II simulation charge. The outer surface of the simulation charge is located at the peak stress contour calculated for the nuclear event corresponding to the detonation pressure of the explosive used for the simulation. Therefore, if normal-density ANFO were used, it would be necessary to reduce the radius of the charge outer contour to correspond to the 90 to 100 kbar peak stress contour. However, the volume enclosed by this contour is so small that sufficient explosive cannot be put into the cavity to match the total impulse along that contour. The situation is made worse by the fact that at this smaller radius more energy is coupled to the ground by the nuclear event, necessitating the use of a larger quantity of explosive for the simulation.

To circumvent this problem a low-density ammonium nitrate/fuel oil explosive with lower detonation velocity and pressure has been developed for use in the MINE THROW II Event. This has been achieved by diluting standard prilled ANFO with low-density styrofoam beads. Because of their low density, the beads

contribute very little mass (typically less than 1 percent) to
the explosive, and therefore should not significantly affect the
detonation reaction. Stable detonations have been achieved in
mixtures with a density as low as 0.5 gm/cm^3 (compared with a
normal ANFO density of 0.86 to 0.90 gm/cm^3).

A survey was made of materials suitable for diluting the
ANFO, and three candidate materials were chosen. These are
listed below with their approximate density and cost.

Diluent	Density	Cost
Styrofoam beads	1 lb/ft^3	\$ 1.50/ft^3
Saran microballoons	2 lb/ft^3	\$10.00/ft^3
Bakelite microballoons	20 lb/ft^3	\$30.00/ft^3

The three candidate diluents were tested and each was found to
have serious disadvantages. The Saran microballoons tend to
clump together and therefore are difficult to mix uniformly with
the ANFO. Also, because of their small individual size, a large
volume of microballoons must be added to significantly reduce
the density of the explosive. A large volume of Bakelite micro-
balloons was also required, although they mixed with ANFO more
easily. Because of the relatively high density of the Bakelite
microballoons a non-negligible mass of material was added to the
explosive, which is undesirable. In both cases the costs were
prohibitively high.

Styrofoam beads have several desirable features. They are
low in density, low in cost, and the volume and mass of material
necessary to lower the explosive density is less than for the
other two diluents. The major problem is that the styrofoam

beads tend to segregate as the mixture is agitated, causing variations in density throughout the mix. However, by mixing the correct proportion of styrofoam beads into each individual bag of ANFO, this effect can be minimized. Although the density of the mixture within the bag may not be uniform, the variations will be on a scale that is small compared to the charge size for MINE THROW II and should not produce a significant effect. This has been verified in the test program described in this report.

SECTION 2

TEST PROGRAM

2.1 SMALL-SCALE FEASIBILITY TESTS

To test the feasibility of using a diluent to produce a low-density ANFO explosive, a series of small-scale tests was performed. The purpose of the tests was to determine the detonability of diluted ANFO mixtures at various densities and to provide preliminary data to help in designing larger tests.

The experimental configuration is shown in Figure 1. The explosive was initiated with a 1-pound pentolite charge and the detonation trajectory along the centerline of the charge was measured with ionization switches. Styrofoam beads were used as the diluent in all tests except one (ρ_0 = 0.71) in which Saran microballoons were used. Densities ranging from 0.5 gm/cm^3 up to a normal density of 0.88 gm/cm^3 were tested and no problem in achieving a detonation was found. The sensitivity of the explosive increased with a decrease in density, and a systematically lower final-detonation velocity was observed for the lower density mixtures. Figure 2 shows values of the final detonation velocity measured at the end of the charge after the detonation had propagated approximately 80 cm. These are plotted as a function of charge density and are compared with an empirical prediction of the steady-state detonation velocity of ANFO (discussed later in this report). Figure 3 shows a comparison of detonation trajectories in three different density mixtures. It is clear from this figure that the detonation velocity is still increasing and that a larger charge size is necessary to determine the steady-state detonation velocities.
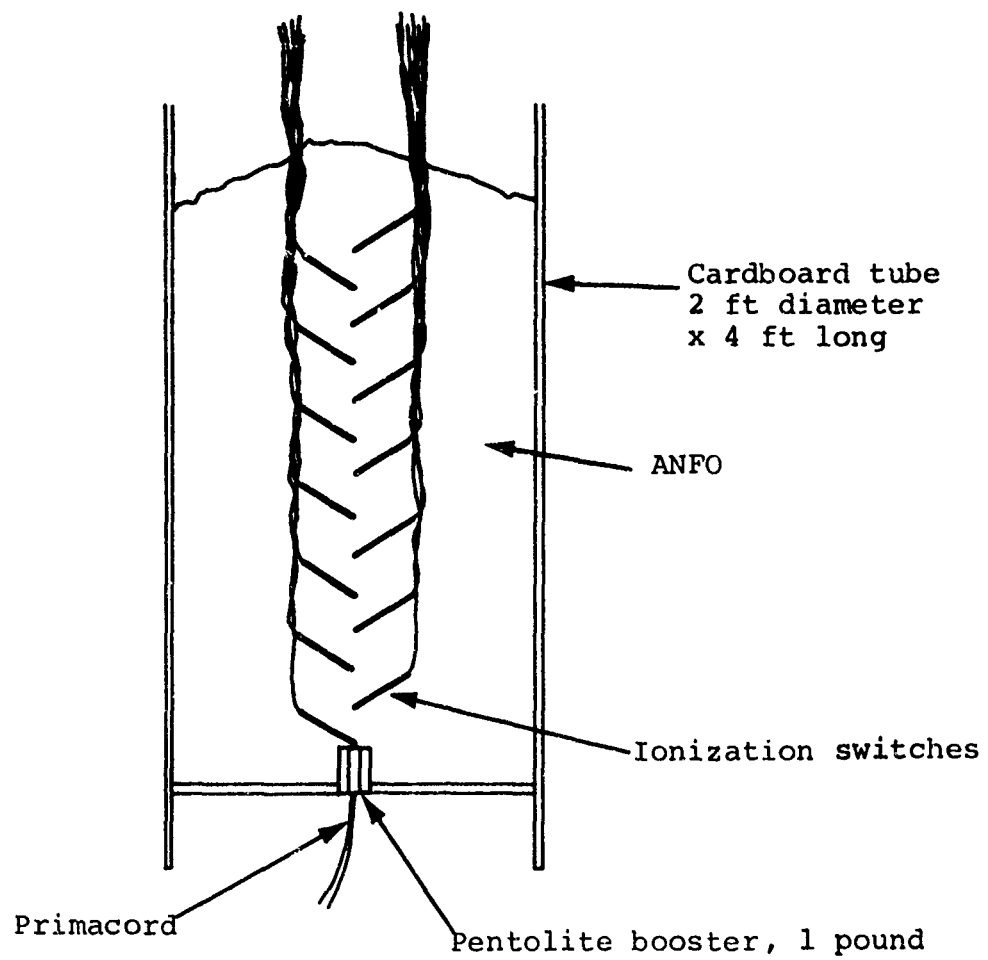
Figure 1   Experimental configuration for small-scale detonation tests of low density ANFO.
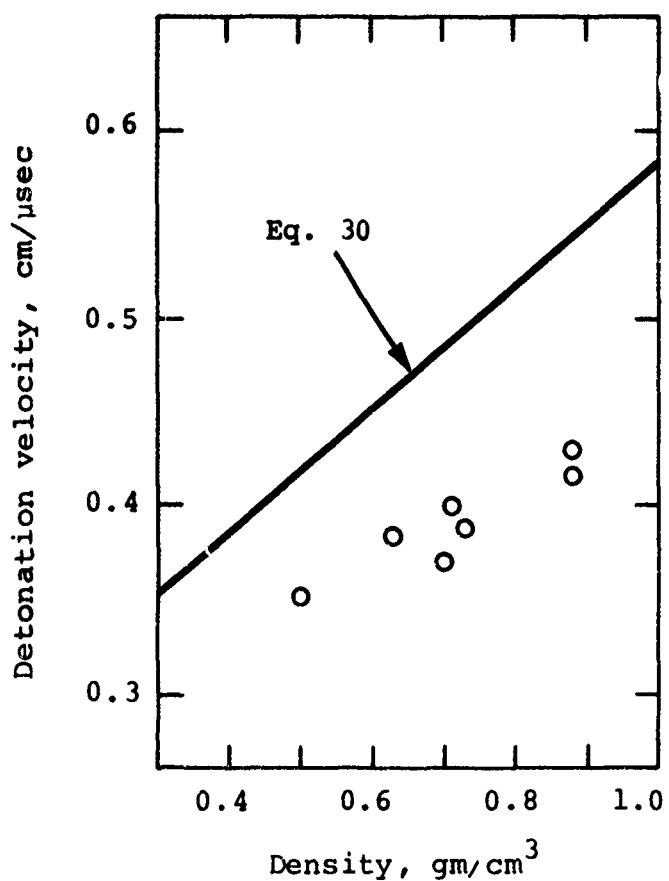
Figure 2   Final detonation velocities for small-scale tests of
            diluted ANFO.

11

300

D_f (cm/μsec)

□ ← 0.35

△ ← 0.39

← 0.43

Time, μsec

200

○ ρ_o = 0.88 (undiluted)

△ ρ_o = 0.73

□ ρ_o = 0.50

100

0   10   20   30   40   50   60   70   80   90   100

Distance, cm
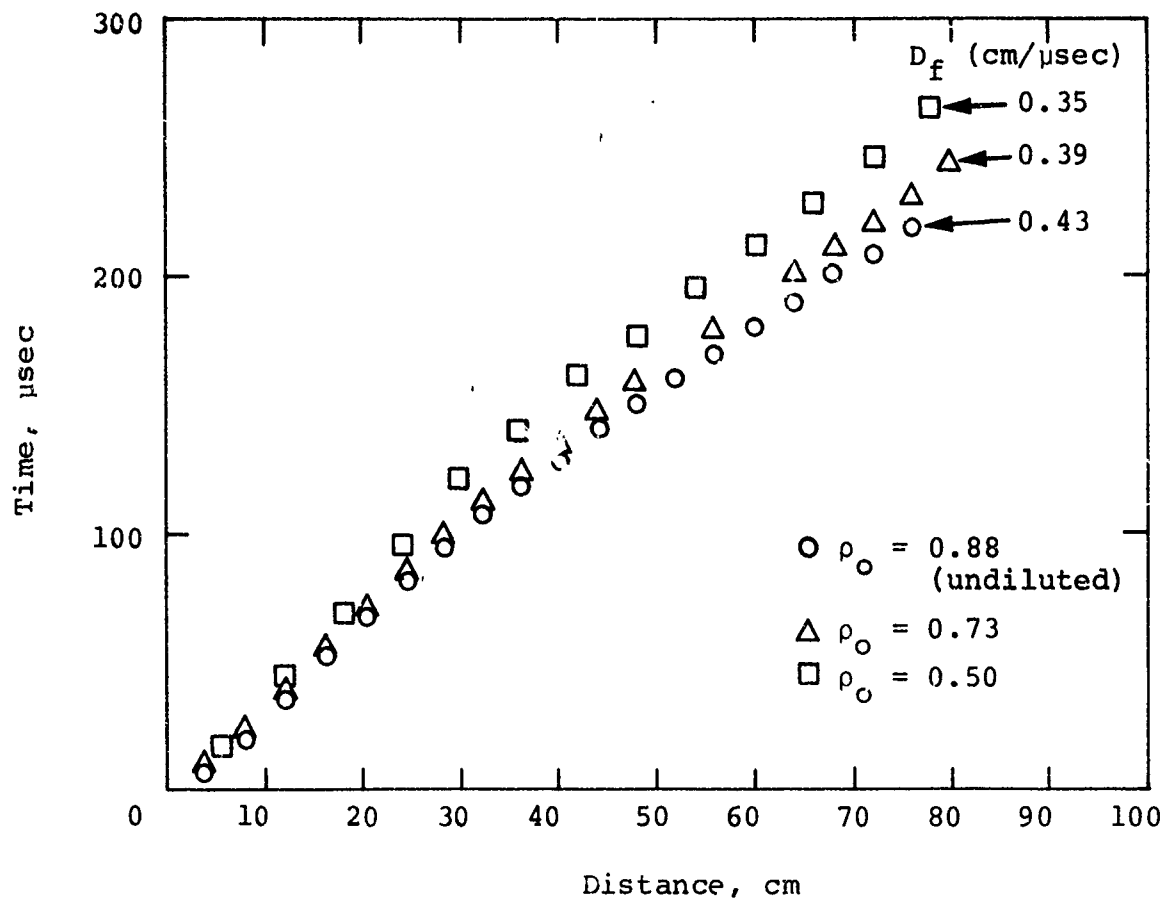
Figure 3   Detonation trajectories for three small-scale diluted ANFO tests.

12

2.2 LARGE-SCALE TESTS

To determine the steady-state detonation characteristics of diluted ANFO as a function of density, a series of large-scale tests were conducted at the Nevada Test Site. The test configuration, shown in Figure 4, consisted of an 8-foot cube of explosive detonated on one side by an array of pentolite charges simultaneously initiated to produce a planar detonation front. The array of initiators is shown in Figure 5. The ANFO charge was constructed from bags of the diluted ANFO mixture of a size equivalent to a 50-pound bag of undiluted ANFO. Figure 6 shows the weight of ANFO per bag as a function of average charge density of the five tests conducted. Also shown is the volume of styrofoam beads added per bag for those five tests. Figure 7 shows a typical bag of the diluted ANFO mixture. It is clear that a significant fraction of the styrofoam beads has become segregated at the surface of the bag. The effect of this incomplete mixing can be observed in the detonation trajectories and will be discussed later. The detonation velocity was measured with an array of ionization switches oriented as shown in Figure 4. The switches were taped to a sheet of Mylar to assure proper positioning (Figure 8) and the entire assembly was placed in the charge as it was being stacked (Figure 9). Signals from the ionization switches were recorded on raster oscilloscopes and from those records a time history of the detonation front was determined for each test. Manganin pressure gauges were mounted on the surface of the charges opposite the initiators in an attempt to measure the detonation pressure. However, on all five tests the gauges broke before a peak stress could be recorded, and no data were obtained. A new gauge design must be developed and tested prior to MINE THROW II to insure that pressure measurements are obtained for that test.

13
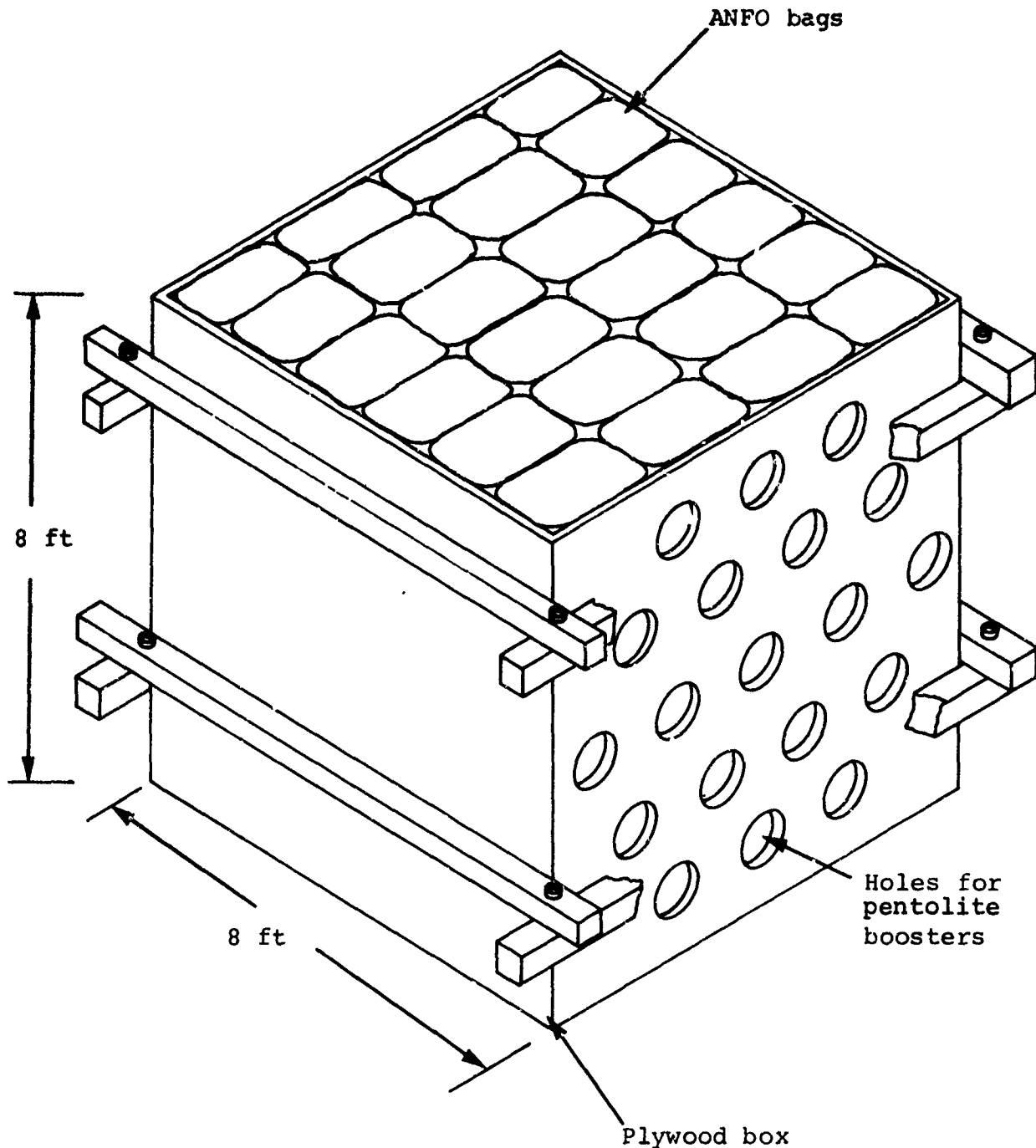
Figure 4   Test configuration for the large-scale detonation
             tests of diluted ANFO.
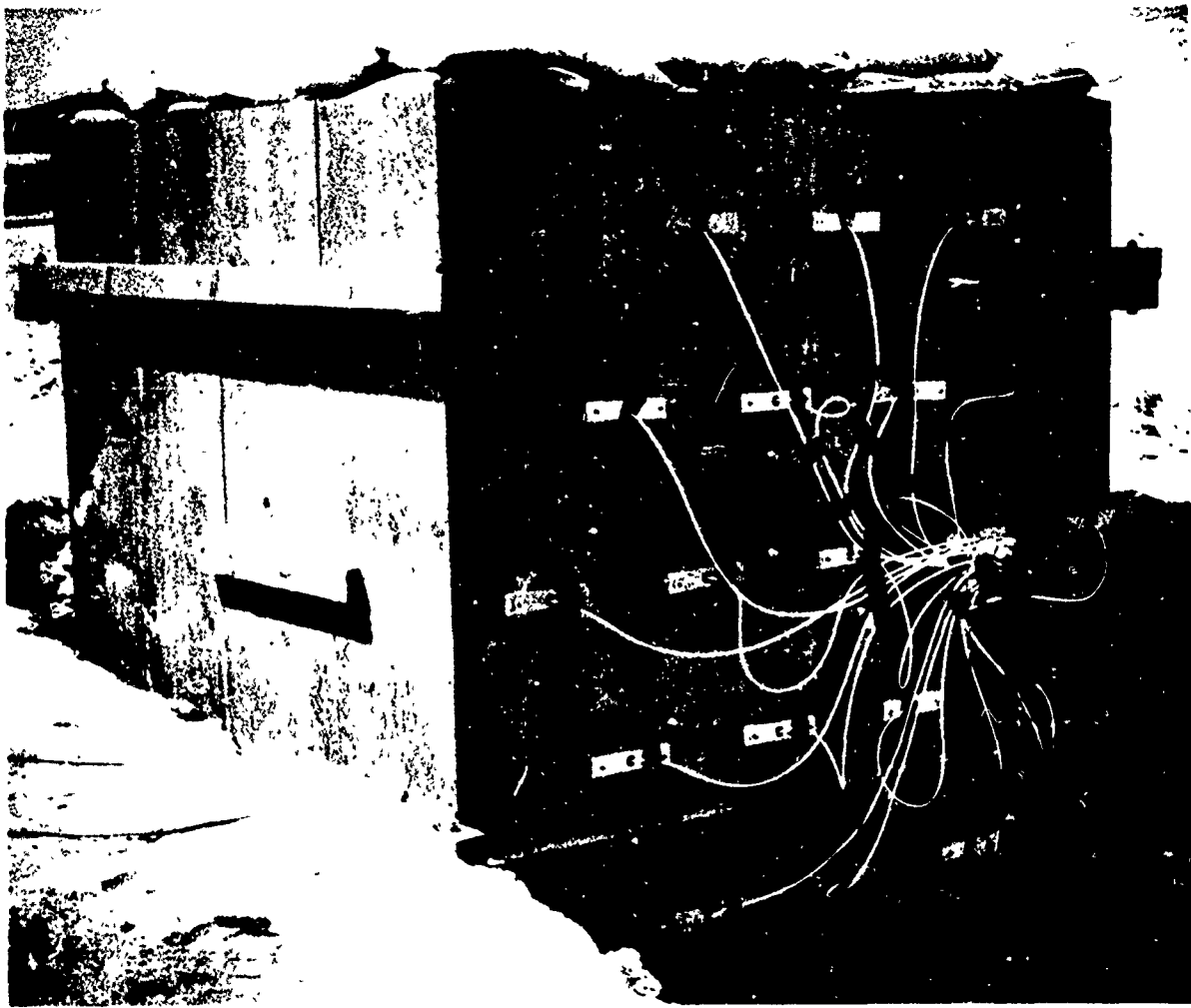
Figure 5 Array of initiators.

A2580

15
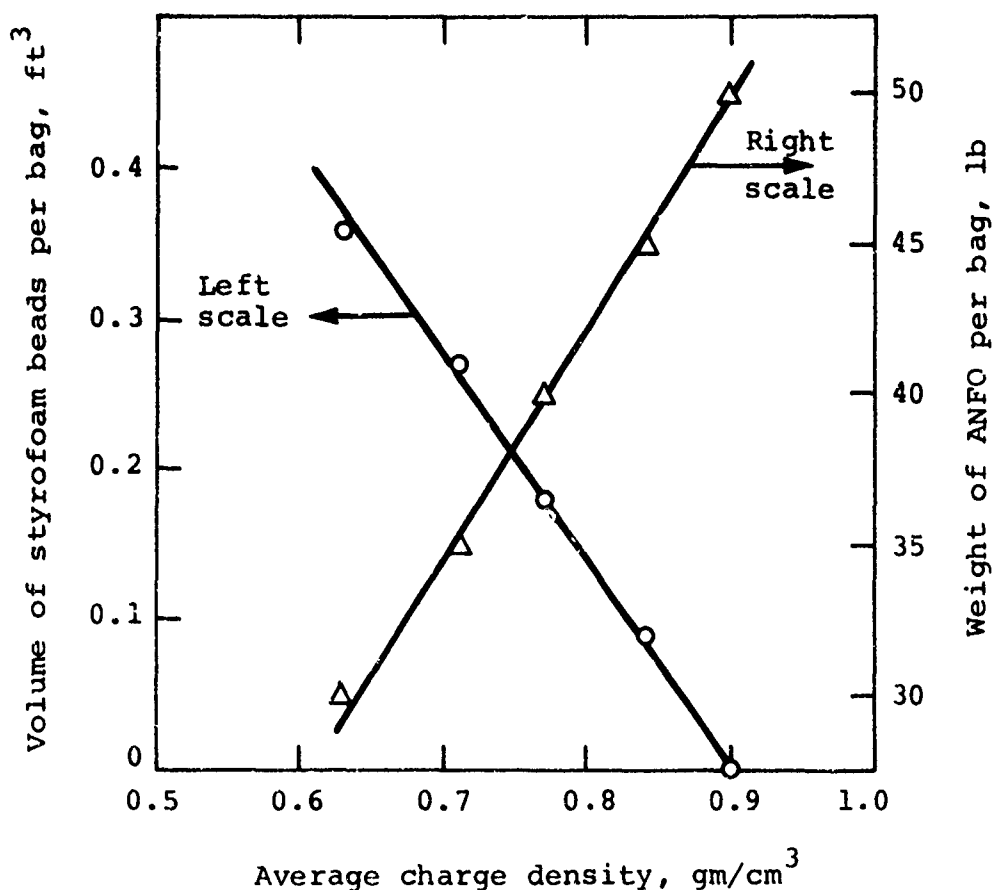
Figure 6   Weight of ANFO and volume of styrofoam beads combined
per bag as a function of charge density for the
large-scale diluted ANFO tests.

16

Figure 7 Typical bags of diluted ANFO mixture.

A1366

Figure 8 Positioning of the ionization switches prior to installation.

18

A1364

Figure 9   Installation of the ionization switches in the charge.

One plausible explanation for gauge failure on all the tests is the possible existence of a very irregular, nonplanar detonation wave front in the ANFO. Because of the heterogeneous nature of the diluted ANFO an irregular wave front is likely, and small jets may even form at the front as a result of the interaction of the ANFO prills and the polystyrene beads. As this irregular front impinges on the manganin gauge element, large deformations could be produced, causing failure.

If this is the cause of the gauge failure, it can be circumvented by placing a thicker buffer between the explosive and the gauge element. A layer of plexiglass, or some other suitable material on the order of 1 to 2 inches thick covering the front surface of the gauge, will allow the irregularities in the shock front to smooth out before reaching the gauge.

The detonation trajectories measured in these tests are shown in Figures 10 through 14. In all cases, the detonation velocity increases with propagation distance until a constant value is achieved at a distance somewhere between 100 and 150 cm. The trajectories are more irregular than those measured in the small-scale tests; the irregularity increases with increased dilution of the explosive and exhibits a periodic structure that has a characteristic length about the same as the length of a bag of explosive. The irregularities in the detonation trajectories are probably caused by the incomplete mixing of the ANFO and the styrofoam beads within each bag. Although the effects are probably not important, to prevent any future problems a better mixing technique should be developed for the MINE THROW II explosive.

20
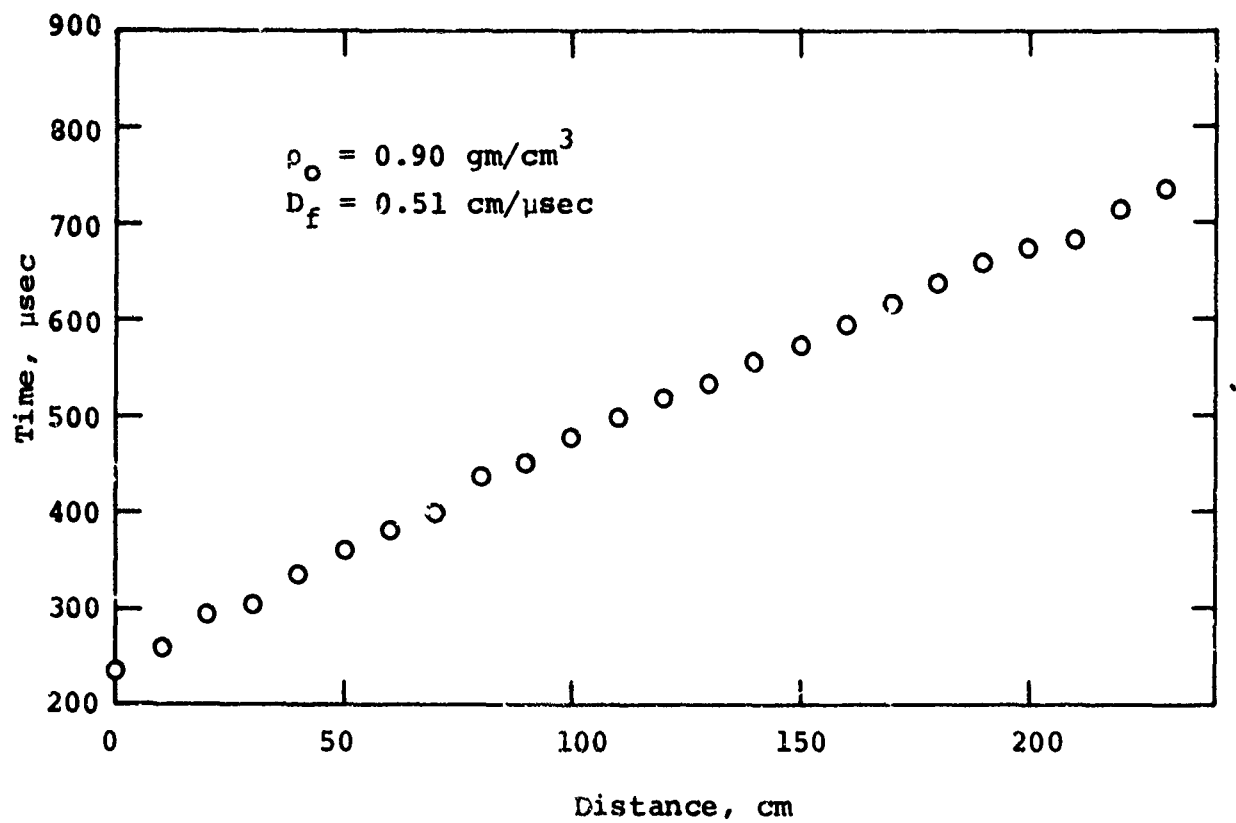
Figure 10   Detonation trajectory for undiluted 94/6 ANFO.

$\rho_o = 0.82$ gm/cm^3

$D_f = 0.465$ cm/μsec
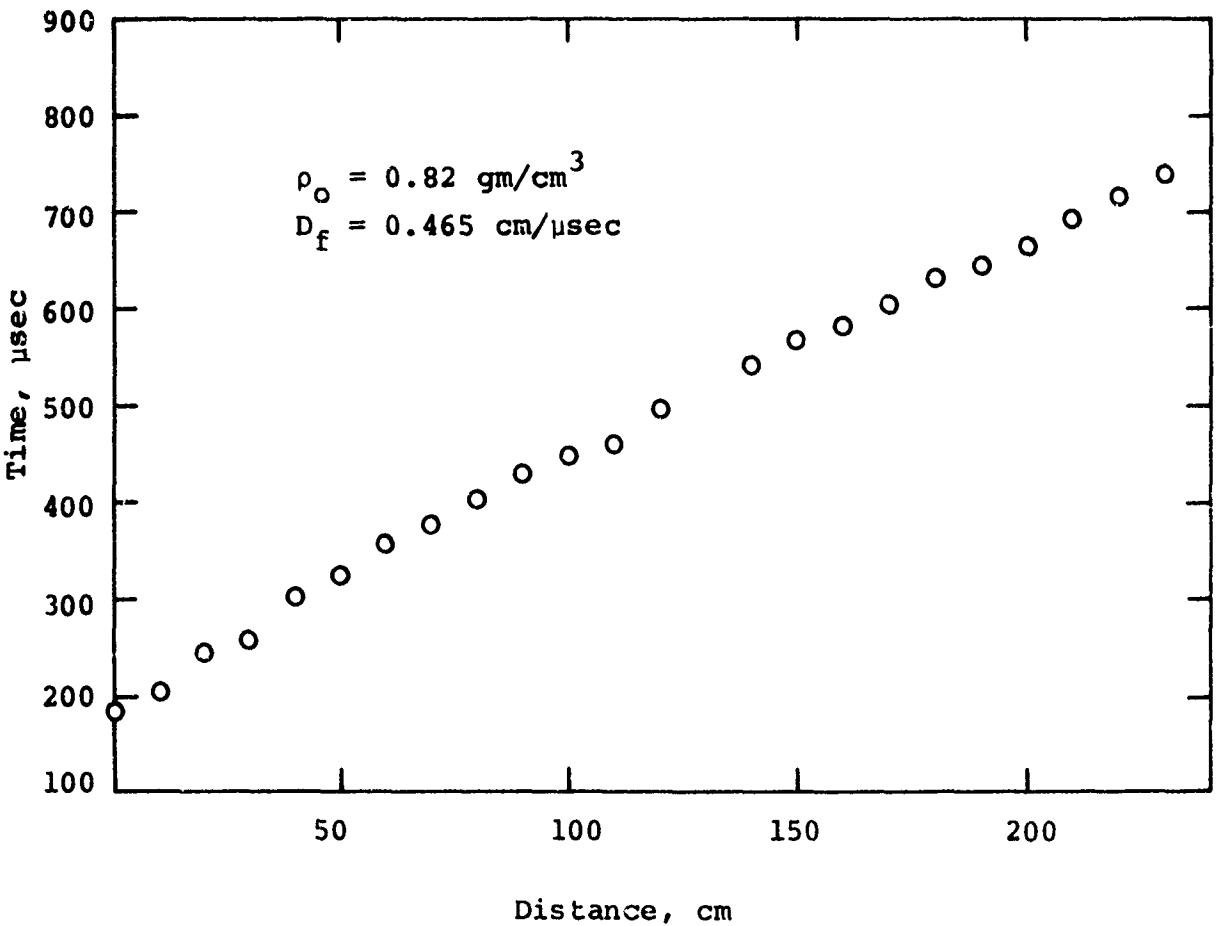
Figure 11   Detonation trajectory for diluted ANFO.
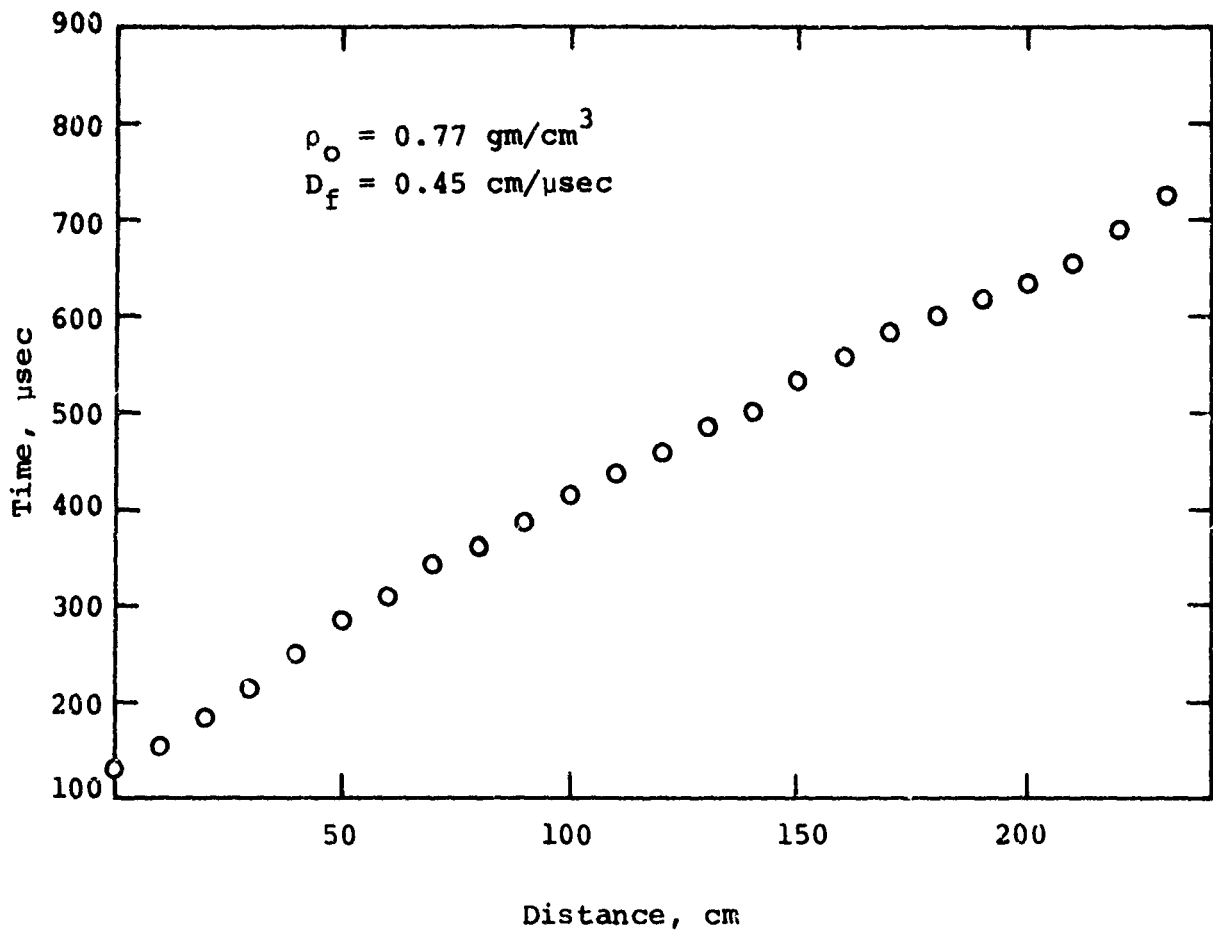
Figure 12   Detonation trajectory for diluted ANFO.
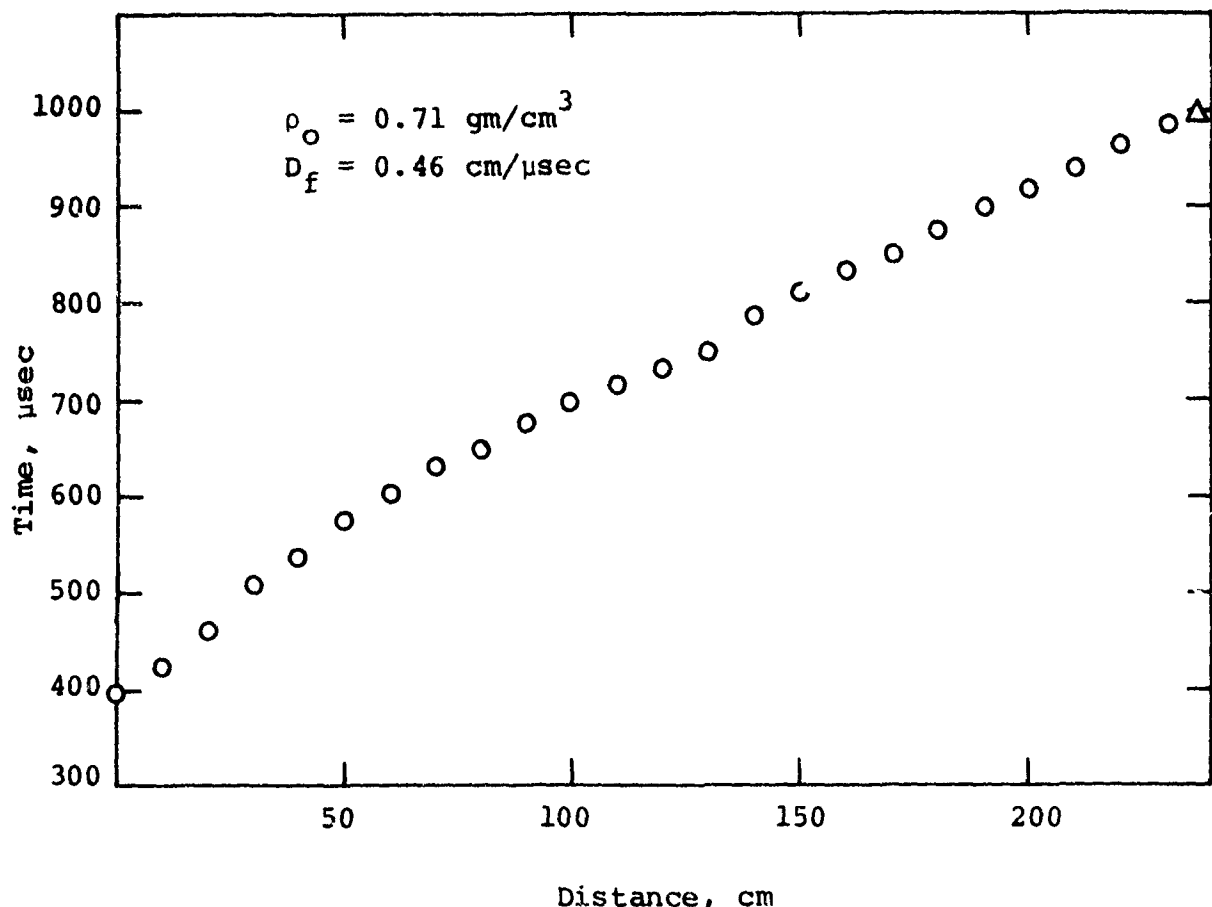
Figure 13   Detonation trajectory for diluted ANFO.
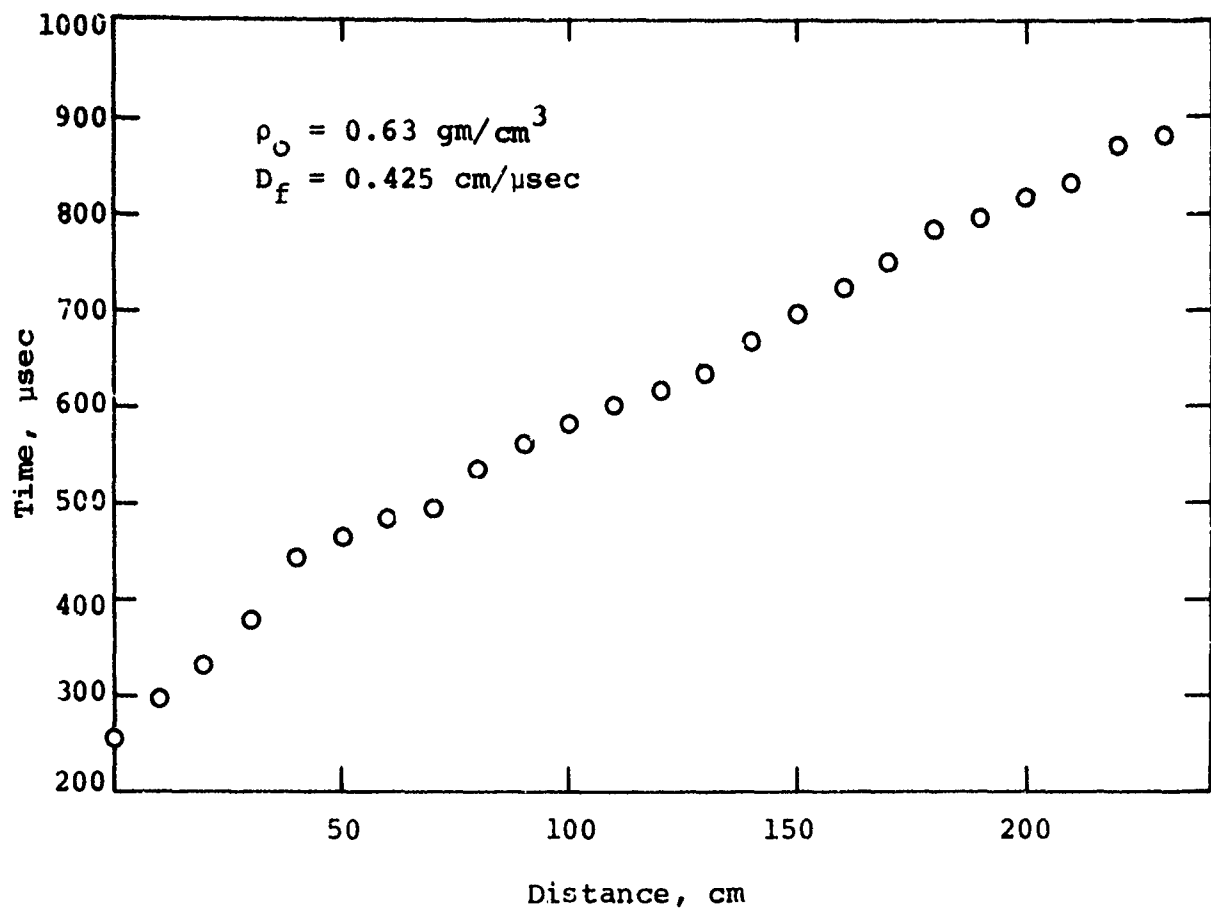
Figure 14   Detonation trajectory for diluted ANFO.

$\rho_O = 0.63$ gm/cm^3

$D_f = 0.425$ cm/µsec
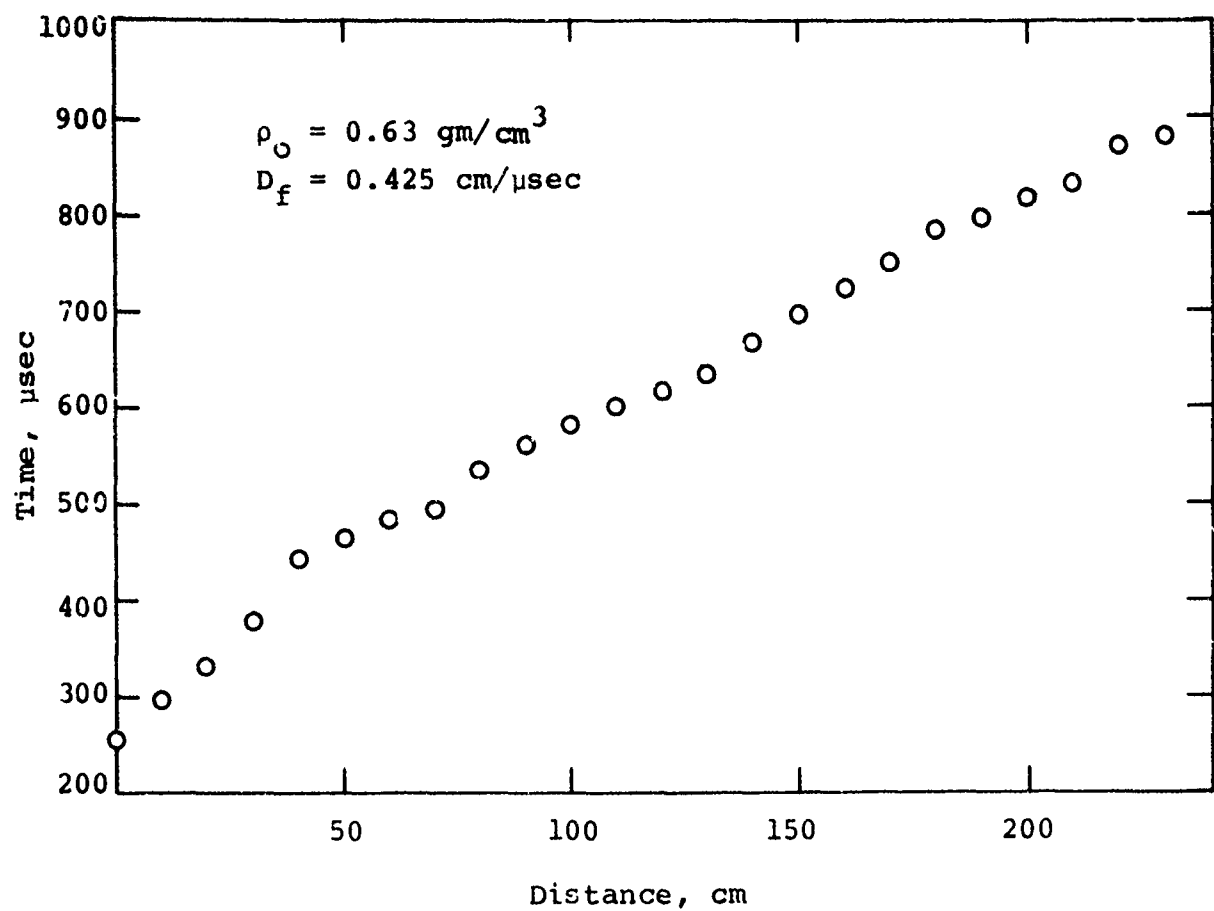
Figure 14   Detonation trajectory for diluted ANFO.

Figure 15 shows a composite graph of the detonation trajectories for the five large-scale tests. The comparison shows a consistent trend toward lower detonation velocities throughout the trajectory for lower density explosives. From these data, a mixture having a density on the order of 0.7 to 0.75 gm/cm^3 was selected for the MINE THROW II Event.

To design the MINE THROW II charge, a mathematical model describing the detonation behavior of the low-density ANFO was developed from these data to be used in the finite-difference calculations of the charge performance. Details of the development of this model and the underlying theory are presented below.
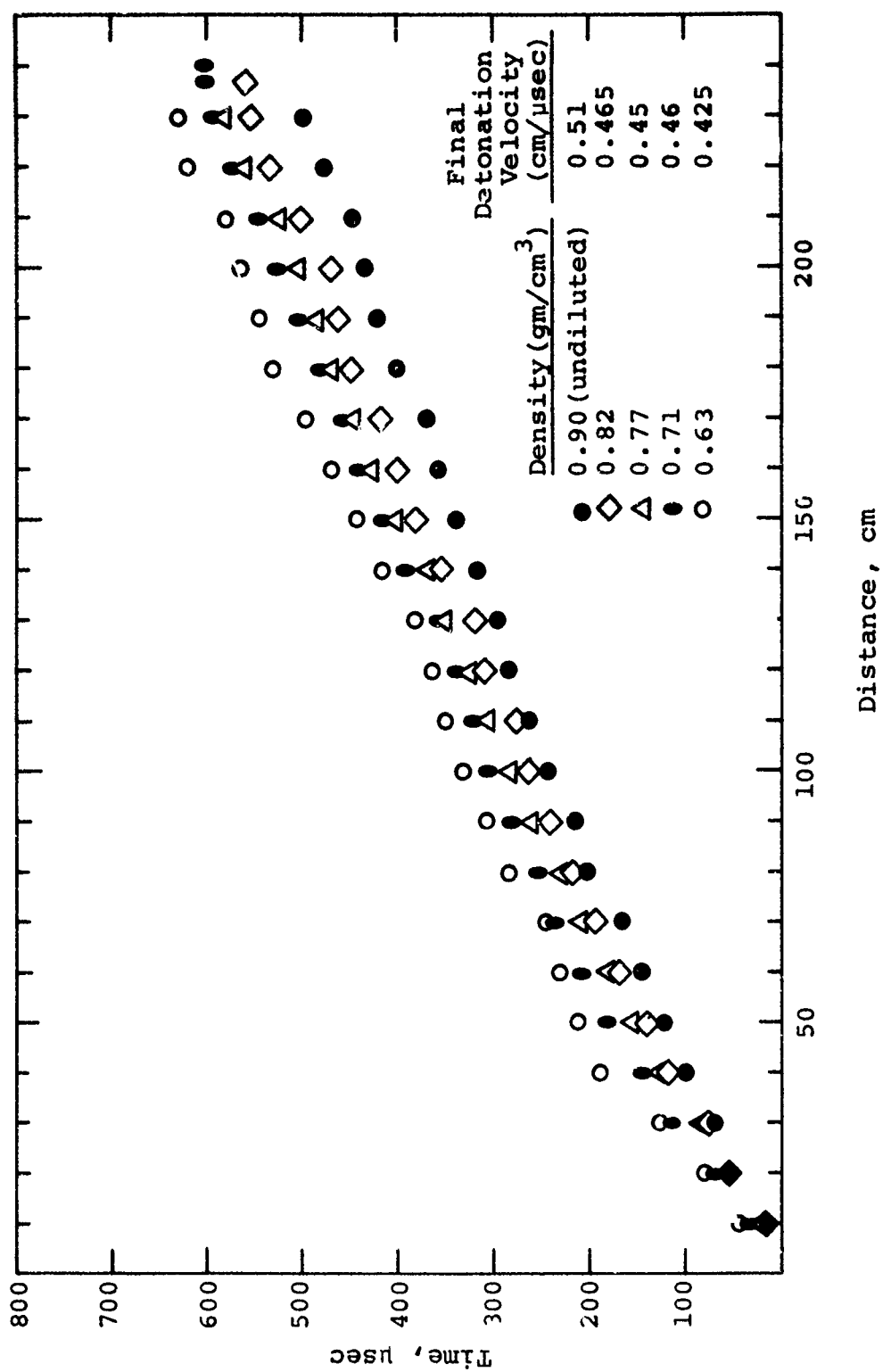
Figure 15   Detonation trajectories for diluted ANFO.

27

SECTION 3
MODELING OF DETONATION PROPERTIES

3.1 CHAPMAN-JOUGUET DETONATIONS

A detonation is generally represented as a strong shock, which suddenly compresses and heats the unreacted explosive, followed by a reaction region within which the explosive energy is released. This is shown schematically in Figure 16. The reaction takes place over a finite time, τ, within a reaction zone of width a. The energy released within this zone provides the potential to maintain the shock front.

In a manner similar to deriving the Hugoniot relations for a steady shock wave in an inert material, the equations expressing conservation of mass, momentum, and energy can be used to relate quantities on either side of the reaction zone for a steady-state detonation. These equations, in the steady-state reference frame moving with the detonation front, are:

$$\rho (D - u) = \rho_o D \tag{1}$$

$$P + \rho (D - u)^2 = P_o + \rho_o D^2 \tag{2}$$

$$E + Pv + \frac{1}{2} (D - u)^2 = Q + E_o + P_o v_o + \frac{1}{2} D^2 \tag{3}$$

where ρ is density, D is the detonation velocity, u is the material velocity, P is the pressure, v is specific volume,
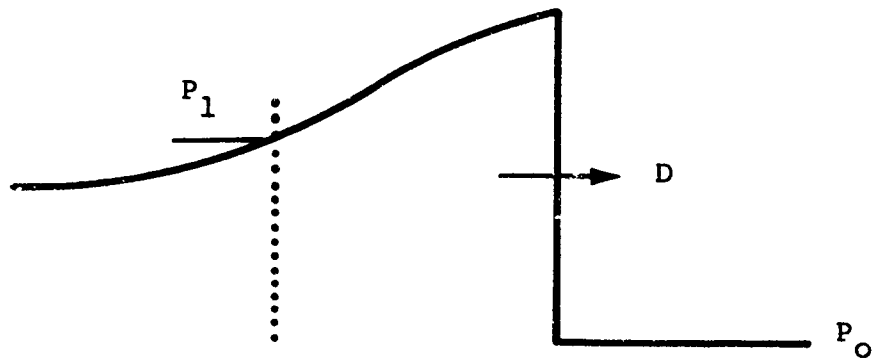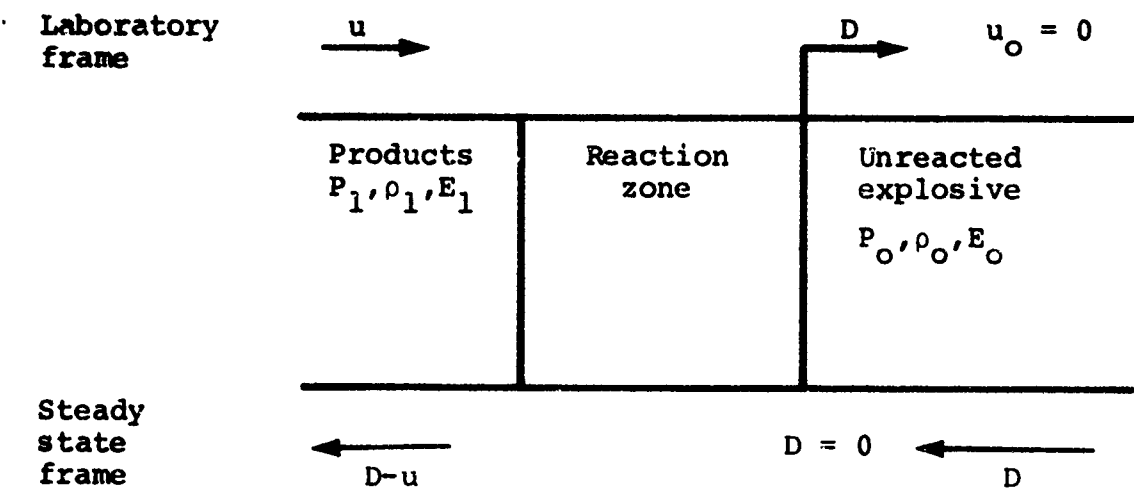
Figure 16   Schematic representation of detonation wave.

E is specific energy, and Q is the chemical potential energy
(heat of reaction). These can be manipulated to give the follow-
ing equations for the variables behind the reaction zone:

$$U = (v_o - v) \sqrt{\frac{P - P_o}{v_o - v}} \qquad (4)$$

$$D = v_o \sqrt{\frac{P - P_o}{v_o - v}} \qquad (5)$$

$$P = P_o + \frac{v_o - v}{v_o^2} D^2 \qquad (6)$$

$$E = E_o + \frac{1}{2} (P + P_o)(v_o - v) + Q \qquad (7)$$

The final expression is the Rankine-Hugoniot equation for a
detonation wave. From these equations and an equation of state
for the detonation products, $P = f(V,E)$, the Hugoniot curve for
the detonation wave can be defined. This is shown in Figure 17.
It can be shown (Reference 5) that a stable steady-state detona-
tion corresponds to a unique state (P_1, v_1) on the detonation
Hugoniot for which the detonation wave speed D is equal to the
sound speed (relative to the laboratory frame) in the reaction
products. This condition

$$D = u + C \qquad (8)$$

was proposed independently by Chapman and Jouguet and is known
as the Chapman-Jouguet condition. The state P_1, v_1 is known as
the Chapman-Jouguet state. An equivalent condition is that the
Rayleigh line for the detonation wave be tangent to the Hugoniot
of the products as shown in Figure 17 (Reference 5).
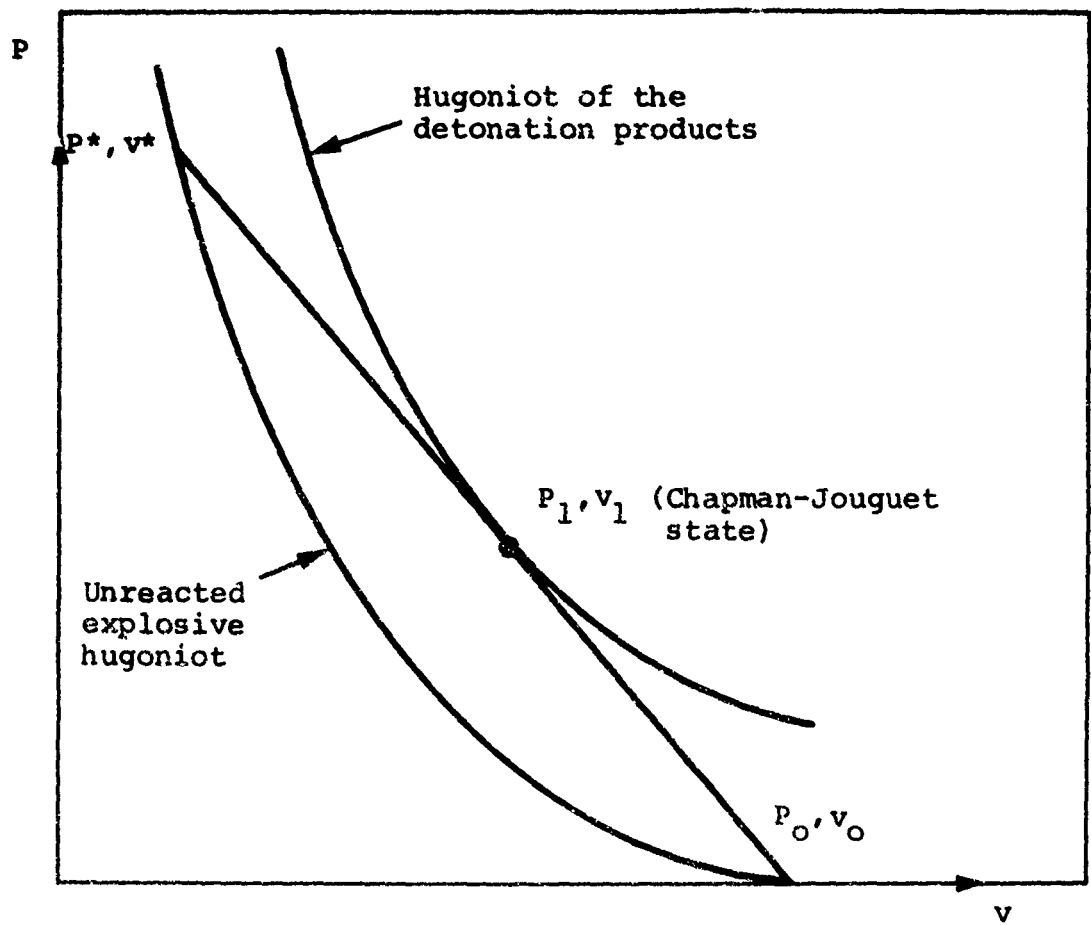
Figure 17   Schematic representation of a detonation in the
pressure-volume plane.

If the equation of state of the products is assumed to be that of a polytropic gas

$$P = (\gamma - 1) \rho E \qquad (9)$$

then Equations 4 through 9 can be used to define the variables at the Chapman-Jouguet state (ignoring P_o relative to P_1):

$$P_1 = 2(\gamma - 1)\rho_o Q = \frac{\rho_o D^2}{\gamma + 1} \qquad (10)$$

$$D = \sqrt{2(\gamma^2 - 1)Q} \qquad (11)$$

$$u_1 = \sqrt{\frac{2(\gamma - 1)}{\gamma + 1} Q} = \frac{D}{\gamma + 1} \qquad (12)$$

$$v_1 = \frac{\gamma}{\gamma + 1} v_o \qquad (13)$$

$$C_1 = \frac{\gamma}{\gamma + 1} D \qquad (14)$$

These equations are not restricted to a polytropic gas description of the products, but hold in general when γ is defined as

$$\gamma_{CJ} = -\left(\frac{\partial \ln P}{\partial \ln V}\right)_s \qquad (15)$$

determined at the Chapman-Jouguet state.

33

In a detonation wave the Chapman-Jouguet state is not
reached instantaneously but after a reaction time τ. According
to an idealized theory, the unreacted explosive is shocked
initially to some state P^*, v^* shown in Figure 17. The chemical
reaction takes place over a time τ with the products reaching
state P_1, v_1 as the reaction goes to completion. The state
P^*,v^* corresponds to the Von Neumann spike at the detonation
front which has never been observed experimentally. In real
detonations, that state may never be reached because of dissipa-
tive effects (e.g., viscosity and heat conduction) in the shock
front (Reference 6).

For most conventional military explosives the chemical
reaction takes place very quickly. Since in most applications
times of interest are generally long compared to the reaction
time and the charge sizes are large compared to the reaction
zone width, it is a reasonable approximation to treat the re-
action as instantaneous. However, for a wide variety of ex-
plosives, including blasting slurries, ANFO, and other composite
explosives, this is not true. For a typical fast-reacting
explosive (e.g., HMX, LX-04) the reaction time is on the order
of 0.1 µsec whereas for a typical ANFO mixture (94 percent
prilled ammonium nitrate to 6 percent No. 2 diesel fuel oil) the
reaction time is on the order of 100 sec or greater. In this
case, for most charge sizes of interest, reaction rate effects
must be taken into account.

3.2 REACTION RATE MODELS

One of the simplest models for explosive reactions is the
Arrhenius first-order reaction rate. The first-order rate
equation is (Reference 7)

$$\frac{dF}{dt} = k \, (1 - F) \tag{16}$$

34

where F denotes the mass fraction of the constituents that have
reacted, and hence also the fraction of the total available heat
of reaction released. The Arrhenius expression for the rate
constant is

$$k = Ae^{-E_a/RT} \tag{17}$$

where R is the universal gas constant, T is the temperature, E_a
is the activation energy, and A is the frequency factor for the
reaction. The factor A may depend weakly on temperature accord-
ing to the relation

$$A = BT^{\alpha} \tag{18}$$

where B = constant and $0 \leq \alpha \leq 1$. Here we will consider A
independent of temperature and rewrite (17) as

$$k = \frac{1}{\tau} e^{-E_a/RT} \tag{19}$$

where $\tau = 1/A$ is the characteristic reaction time.

The activation energy represents a potential energy barrier
for the reaction. This is shown schematically in Figure 18 from
Reference 7. When the thermal energy of the reactants is small
compared to E_a, the exponential term in the rate constant is
near zero and the reaction will not proceed. When the tempera-
ture in the explosive increases, due to shock heating, the rate
constant increases and the reaction proceeds.

The first-order rate equation (Equation 16) is primarily
applicable to gaseous, liquid, or homogeneous solid explosives,
i.e., explosives in which the constituents are available for
reaction instantaneously following the initial shock heating.

35

Reaction coordinate
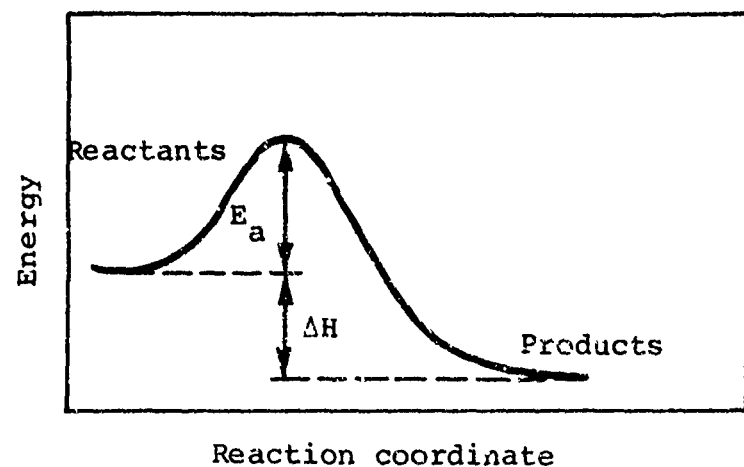
Figure 18   Schematic illustration of activation energy (ΔH = heat of reduction).

36

For ANFO, however, the unreacted explosive is in the form of porous ammonium nitrate prills, approximately 1 to 2 mm in diameter, coated with fuel oil. For the constituents to react the ammonium nitrate prills must first decompose and then mix with the fuel oil. These processes are not taken into account in the first-order rate equation.

Several models have been proposed to describe the reaction process in an ANFO detonation. If one assumes that the decomposition of the ammonium nitrate prill is the controlling process and that the mixing of the decomposition products and the fuel oil takes place essentially instantaneously as the decomposition proceeds, then the grain burning model proposed by Eyring (Reference 8) is a reasonable model. On the other hand, Finger (Reference 9) believes that the decomposition takes place quickly and that the reaction rate is controlled by the diffusion of the reactants. In this work we have considered only the grain burning model.

In the grain burning theory, the rate equation is dependent on the shape of the grains or prills and on the type of ignition. For spherical grains ignited uniformly over the surface, the rate equation is (Reference 10)

$$\frac{dF}{dt} = 3k(1 - F)^{2/3} \tag{20}$$

where k is given again by Equation 19. Under isothermal conditions this may be integrated to give

$$F = 1 - \left(1 - \frac{t}{\tau}\right)^3 \tag{21}$$

where τ is the time for complete reaction. Figure 19 from Reference 11 shows examples of other configurations, i.e., a sphere ignited at the center, a sphere ignited at one point on the surface, and a plane ignited on two sides. It is clear that the amount of reacted material at any given time increases with the number of ignition points. Since these ignition points typically occur at points of contact between grains, for a mixture of spherical prills of ANFO, ignition should occur at several points (typically 6 to 12 according to Reference 11) on the surface. For this case a uniform ignition over the surface is not a bad approximation.

There is a basic difference between the grain burning theory and the first-order rate equation. Grains burn completely in the time τ. According to the first-order rate equation, however, the fraction of reacted constituents increases exponentially to 1 with a characteristic time τ. A comparison of the two models is shown in Figure 20.

To evaluate the effect of the activation energy and the reaction time constant for both this first-order rate model and the spherical grain burning model, a series of finite-difference calculations was performed with the one-dimensional POD code. Finite-difference representations of Equations 16 and 20 were programmed into the POD code with the rate constant, k, given by an equation equivalent to Equation 19. For convenience, the activation energy E_a in Equation 19 was defined by a dimensionless fraction, α, according to

$$E_a = \alpha Q \qquad (22)$$

38
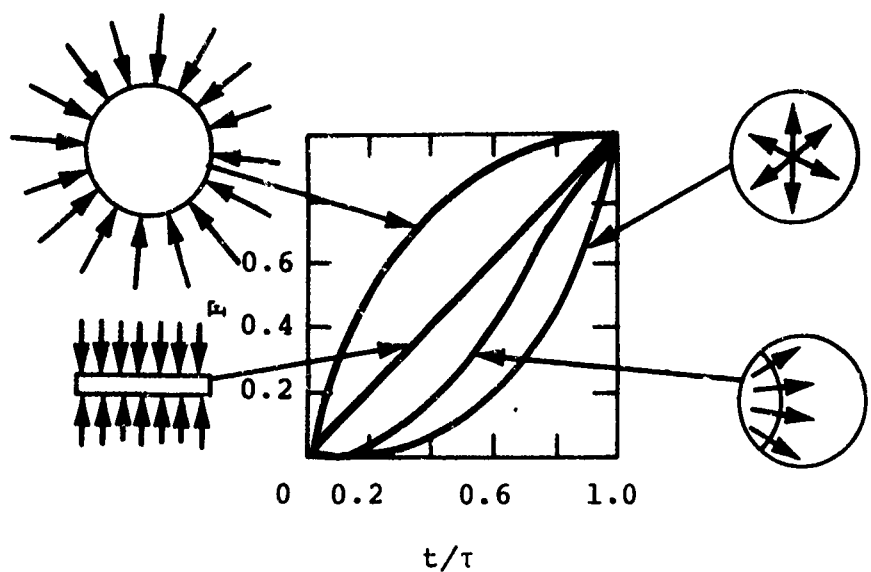
Figure 19   Burning rate for various models (from Reference 11).
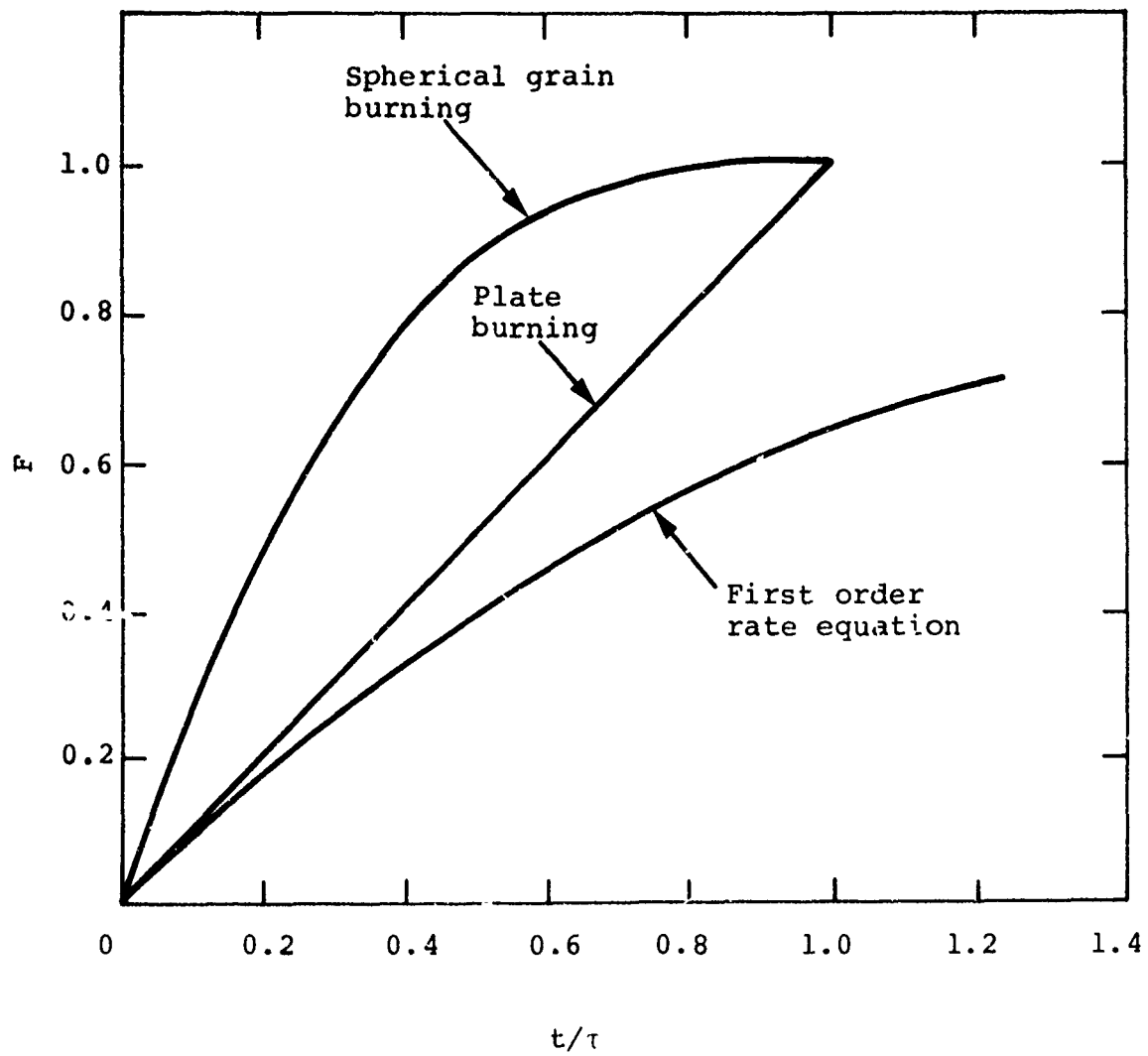
Figure 20   Comparison of isothermal burning for various rate
            models.

40

and Equation 19 was rewritten,

$$k = \frac{1}{\tau} e^{-\alpha Q/E} \qquad (23)$$

where, again for convenience in programming, the factor RT has been replaced by the internal energy E.

A series of one-dimensional (plane symmetry) calculations was made with the first-order rate model to evaluate the effects of variations in the activation energy parameter, α, and the time constant, τ. In all cases, the steady-state detonation properties were the same; so the final values of detonation velocity should be the same. Detonation front trajectories for several values of α are shown in Figure 21. This figure shows that the value α is most important to the initiation of the detonation and has little effect once the full detonation wave has developed. As α increases the detonation builds up more slowly until for $\alpha \gtrsim 0.5$ detonations could not be initiated. Values of α between 0.01 and 0.1 gave good results for calculations of ANFO detonations.

Figure 22 shows detonation trajectories computed with different time constants in the first-order rate equation. As expected, long reaction times result in a slow buildup of the detonation wave. For $\tau = 100$ µsec, steady state was never achieved within the propagation distance calculated.

A similar series of calculations was performed using the grain-burning model. Figure 23 shows the effects of variations in τ. The general effect is the same as for the first-order rate model. By adjusting τ, it was possible to fit an experimentally determined trajectory for undiluted ANFO from one of the small-
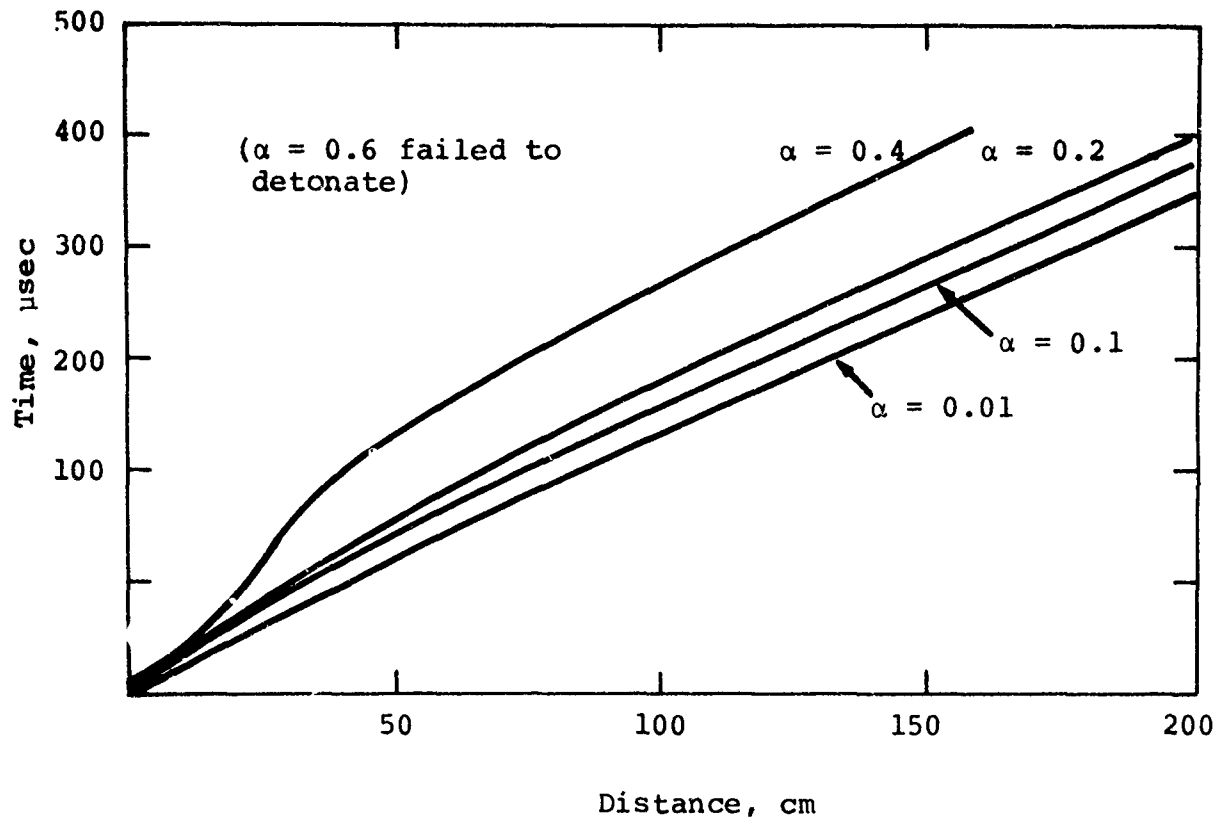
Figure 21   Evaluation of the effect of activation energy on
calculated detonation trajectories for the first-
order reaction rate model (τ held constant = 20 μsec).

42
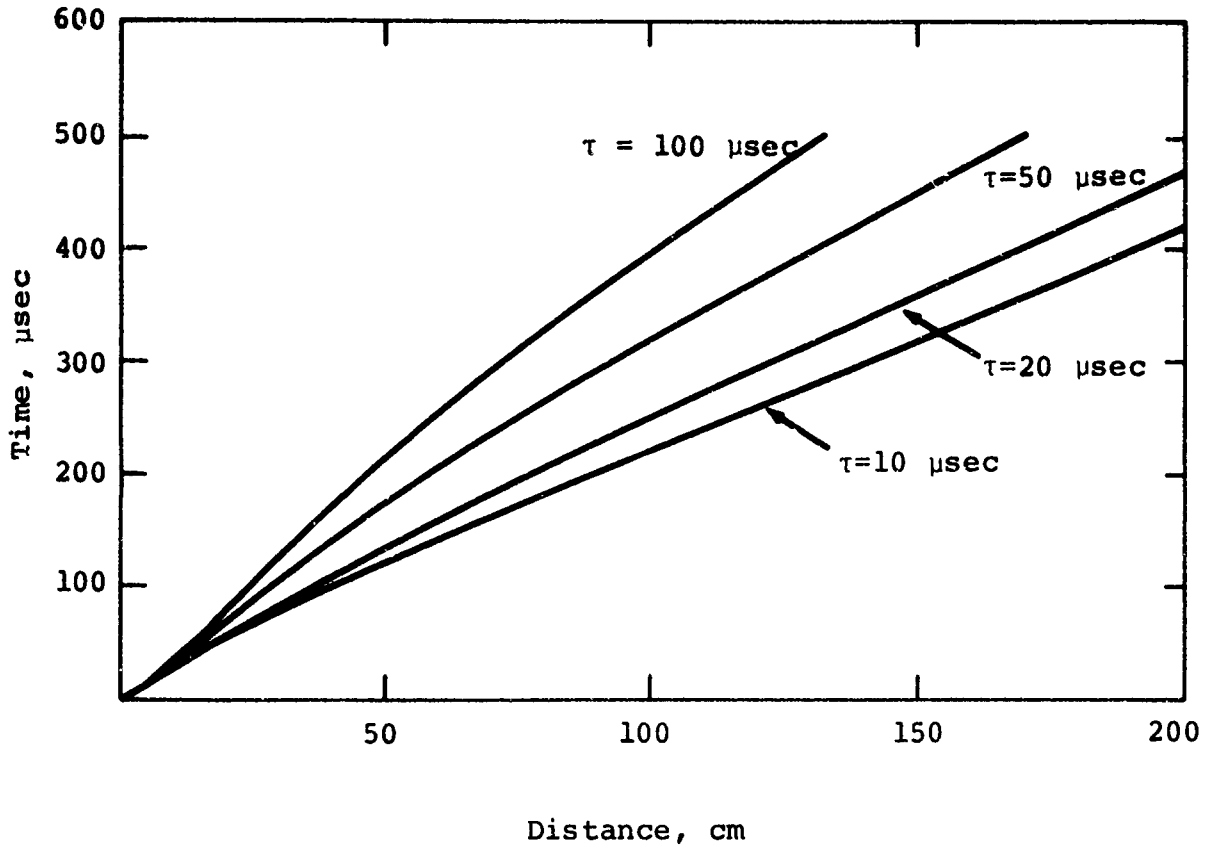
Figure 22   Evaluation of the effect of the reaction time constant, τ, on calculated detonation trajectories for the first order reaction rate model (α held constant = 0.1).

43
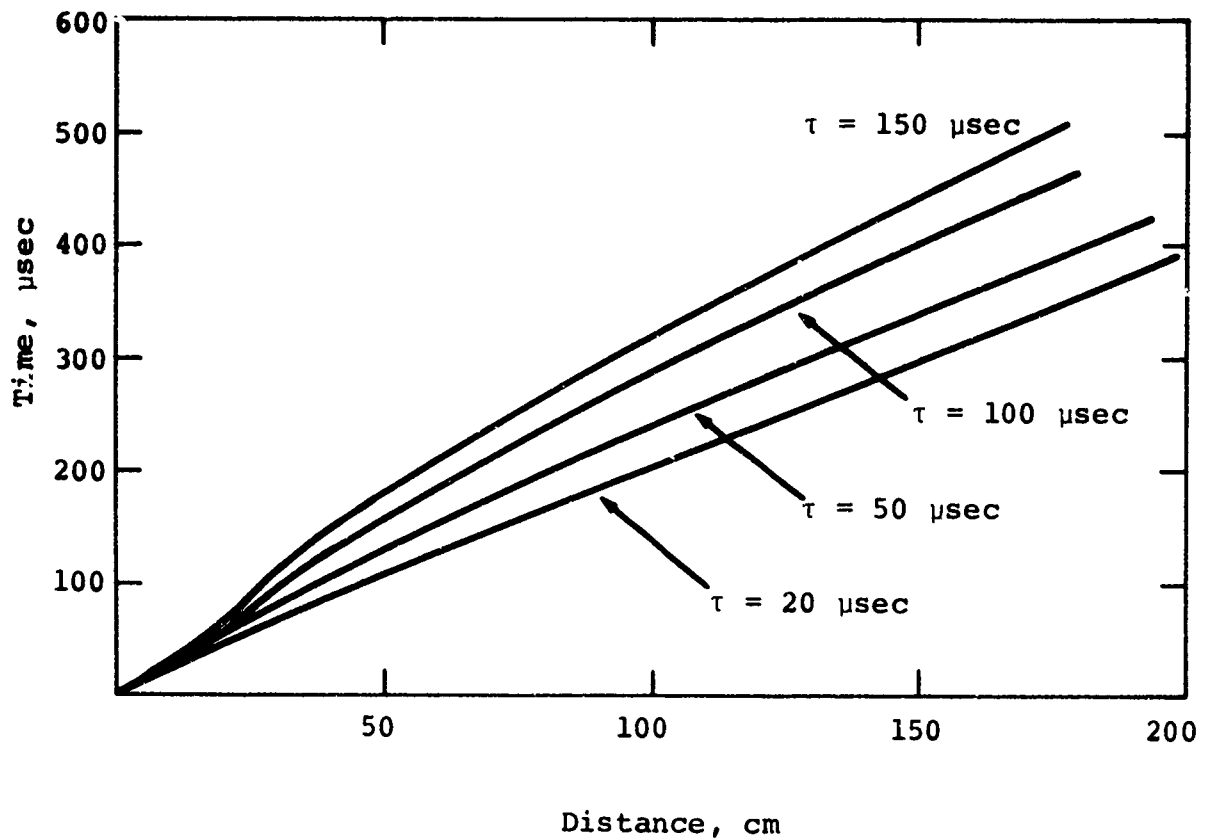
Figure 23   Evaluation of the effect of the reaction time constant, τ, on calculated detonation trajectories for the grain burning model (α held constant = 0.1).

scale tests using this spherical grain-burning model. This is
shown in Figure 24. More comparisons with experiment will be
discussed later.

Typical calculated results of detonation wave buildup for
the two rate models are shown in Figure 25. The pressure builds
up as the detonation approaches steady-state until it reaches a
value higher than the Chapman-Jouguet pressure (P_{CJ}). This peak
corresponds to the Von Neumann spike discussed previously. The
fraction of material reacted is indicated by the dotted line
(related to the scale on the right). As the reaction goes to
completion the pressure drops until it reaches P_{CJ} at the time
that F reaches 1. The calculated spike pressure is not physically
realistic in these calculations. Its magnitude is dependent on
the Hugoniot of the unreacted explosive (see Figure 17), which
was not accurately modeled, and on dissipative effects in the
shock front which were not included here. The Chapman-Jouguet
pressure is probably a better estimate of the actual peak deto-
nation pressure.
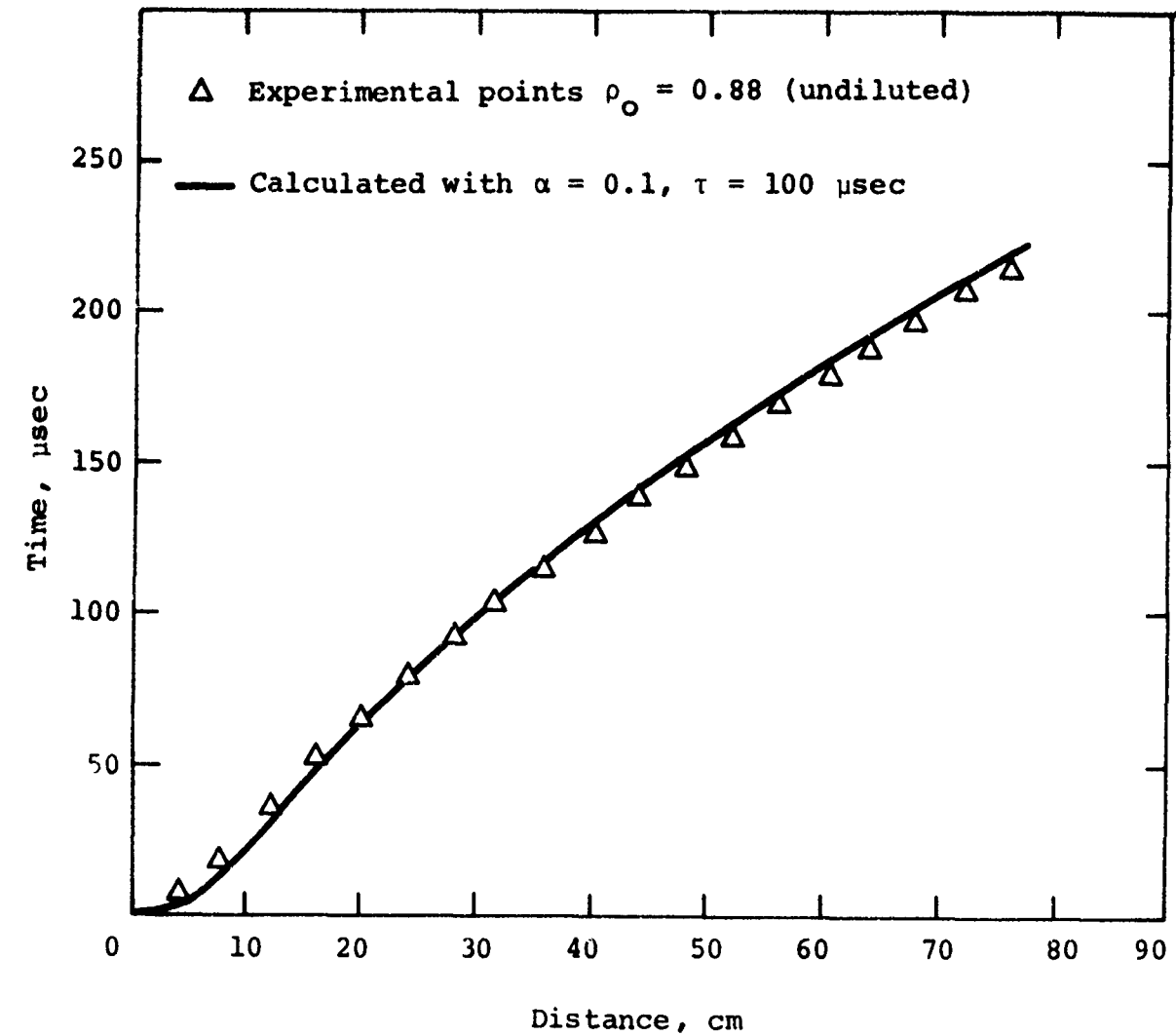
Figure 24   Comparison of measured detonation trajectory with
             calculation using grain burning model.

46
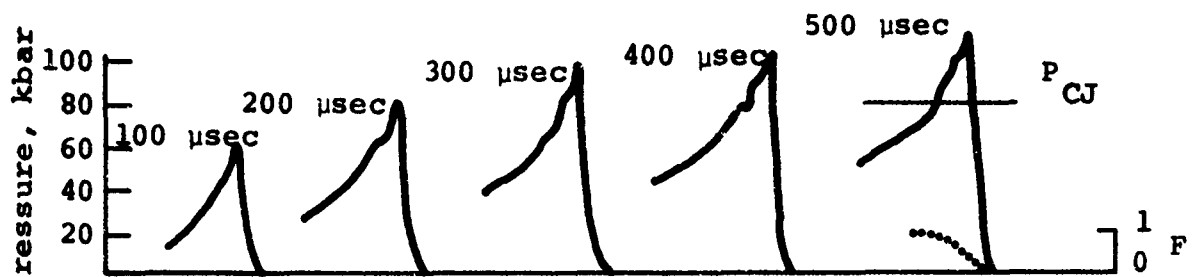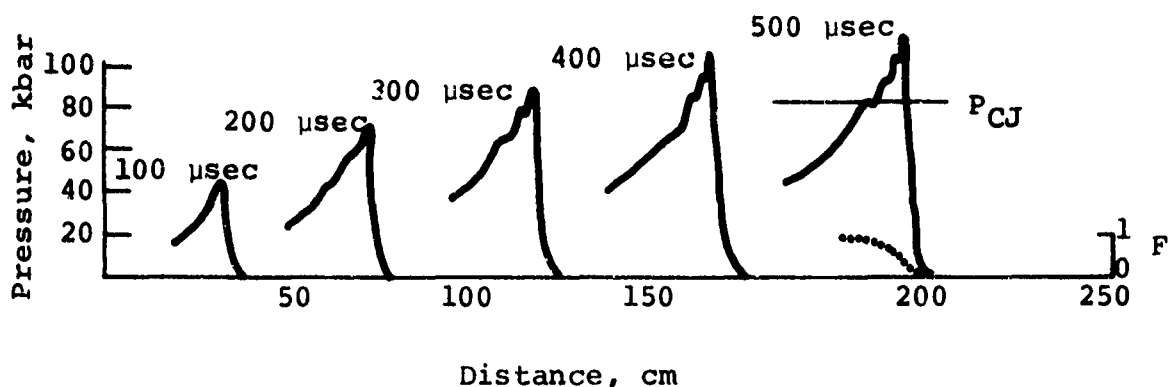
Figure 25   Calculated detonation wave profiles for two reaction
rate models.

SECTION 4

DETONATION PROPERTIES OF
AMMONIUM NITRATE/FUEL OIL EXPLOSIVES

Ammonium nitrate fuel oil mixtures have been widely used as blasting agents for many years in the mining industry and considerable research has been performed to determine their detonation characteristics. This work is summarized in References 10 through 14. While this work was in general quite well done, the investigators were hampered by not being able to experiment with charge sizes large enough to eliminate the effects of the long reaction time. Consequently, detonation velocities and pressure have been predicted that are substantially lower than those measured for large charges.

Recently a number of tests have been conducted using large charges of ANFO. The Naval Ordnance Laboratory (References 15 and 16) conducted tests to determine the airblast characteristics of ANFO compared to TNT; a series of small tests and three large tests(20 to 100 tons) were conducted. Measurements of the average detonation velocity of the charges were made which agreed well with values reported in the literature cited above. Unfortunately, no detailed measurements of the detonation trajectory (or detonation velocity as a function of distance of propagation) were made. On the MINE THROW I event (120 tons) detonation velocities and pressures were measured which were much higher than previously observed (Reference 17). The detonation velocity continued to increase over the entire distance of propagation, reaching a final value of ~ 0.6 cm/μsec. Pressures measured by manganin gauges on the outer surface of the charge were on the order of 90 to 100 kbar.

Although these data disagree with previous measurements, they are the first detailed detonation velocity and pressure measurements made on large ANFO charges and probably are more representative of the steady-state behavior of ANFO. This is supported by data from the test series described in this report and by predictions of ANFO detonation properties based on an empirical method developed by Kamlet et al. (References 1 through 4).

4.1 EMPIRICAL PREDICTIONS

Kamlet and his co-workers have developed a simple empirical method for predicting the detonation properties of C-H-N-O explosives. They have demonstrated that for a wide variety of common military explosives with $\rho_o > 1.0$ gm/cm^3 the method agrees well with data and with the predictions of the RUBY code. Also, Finger (Reference 18) has found that the method agrees well with his data on slurry explosives. The empirical equations are

$$P = K \rho_o^2 \phi \tag{24}$$

$$D = A\phi^{\frac{1}{2}} (1 + B \rho_o)_1 \tag{25}$$

$$\phi = N M^{\frac{1}{2}} Q^{\frac{1}{2}} \tag{26}$$

where K = 15.58, A = 1.01, B = 1.30, P is the detonation pressure in kilobars, D is the detonation velocity in millimeters/μsec, N is the moles of gas per gram of explosive, M is the average molecular weight of the detonation product gases in grams of gas per mole of gas, $Q = -\Delta H_o$ is the chemical energy of the detonation reaction in calories per gram, and ρ_o is the initial density of the explosive in grams per cubic centimeter.

50

Although these equations are generally applicable only for densities above 1.0 gm/cm^3, we have attempted to apply them to ANFO at lower densities. The density restriction comes from an assumption about the reactions

$$2CO \underset{\leftarrow}{\overset{\rightarrow}{{}}} CO_2 + C, \qquad \Delta H_o = -41.2 \text{ kcal} \tag{27}$$

$$H_2 \underset{\leftarrow}{\overset{\rightarrow}{{}}} H_2O + C, \qquad \Delta H_o = -31.4 \text{ kcal} \tag{28}$$
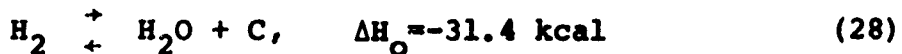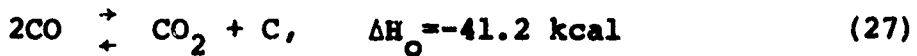
These are assumed to be predominantly to the right which is true only at higher pressure (higher loading densities). However, the reaction considered here (Equation 29 below) is oxygen balanced so that no free carbon exists in the products and the above reactions do not occur. Therefore, the equations should be valid for ANFO at lower densities.

To calculate the detonation properties of ANFO we assume the following reaction (for a stoichemetric mixture of 94 percent ammonium nitrate and 6 percent No. 2 diesel fuel oil):

$$3NH_4NO_3 + CH_2 \rightarrow 3N_2 + 7H_2O + CO_2 \tag{29}$$
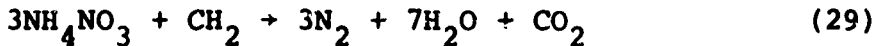
For this reaction $N = 1/M = 0.0433$ moles/gm, $Q = 912$ cal/gm. The resultant equations for detonation velocity and pressure are

$$D(mm/\mu sec) = 3.292 \, \rho_o + 2.532 \tag{30}$$

$$P = 97.95 \, \rho_o^2 \tag{31}$$

which are plotted in Figure 26 for the range of densities of interest here.
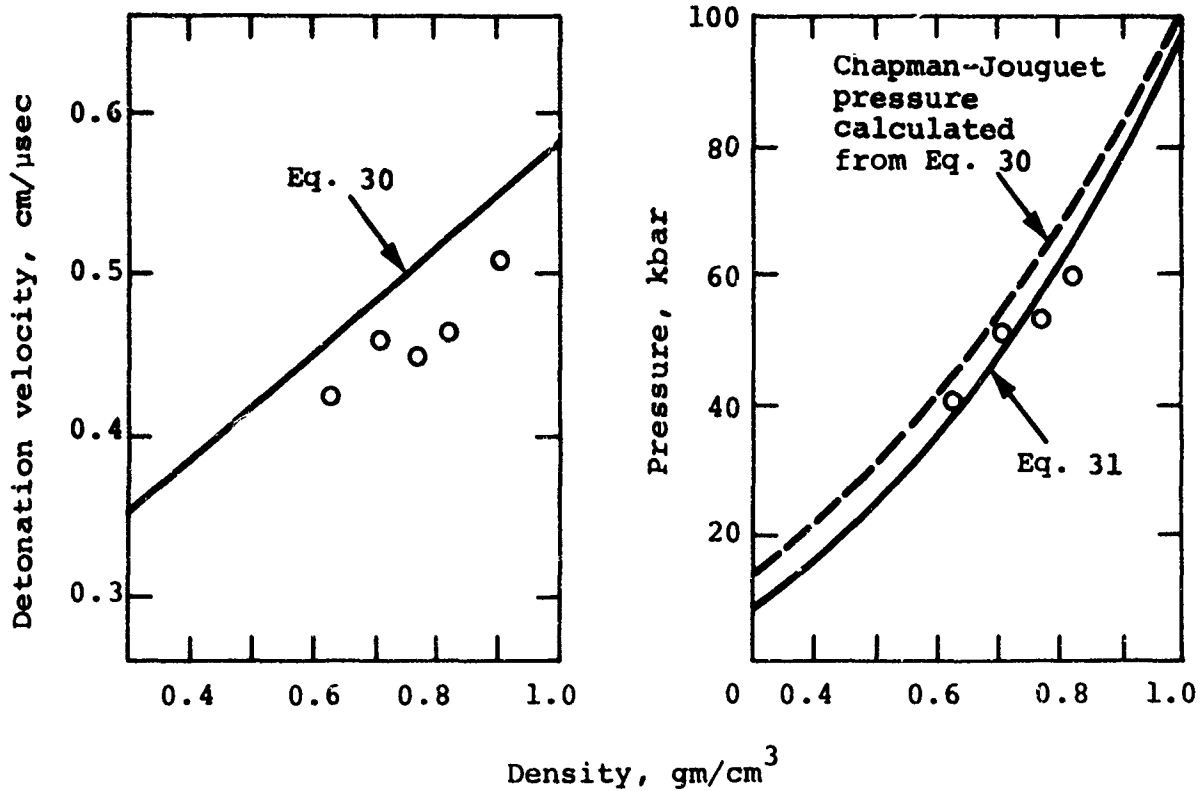
Figure 26   Predicted detonation properties of 94/6 ANFO compared
with measured values.

The Chapman-Jouguet pressure (calculated by solving Equations 10 and 11 for P as a function of D, assuming Q = 912.8 cal/gm) corresponding to the detonation velocity determined by Equation 30 is shown as a dashed line for comparison. The empirical equation predicts slightly lower detonation pressures than would be predicted by Chapman-Jouguet theory.

4.2 COMPARISON WITH EXPERIMENT

Figure 26 also shows a comparison of the predictions with data from the series of large-scale tests of diluted ANFO. The detonation velocities are the final values after steady-state had been achieved, and the pressures are the calculated Chapman-Jouguet pressures corresponding to those detonation velocities. The measured detonation velocities are on the order of 10 percent lower than the predicted values while the pressures are generally in slightly better agreement.

The agreement between measured and calculated detonation velocities is not as good as was reported in Reference 4 for other explosives. There are several factors that could be responsible for this. First of all, our contention that the technique can be used for $\rho_o < 1.0$ gm/cm^3 for ANFO may be incorrect; perhaps there are other factors not considered that make the technique invalid in this range. Secondly, the explosives to which the technique was applied in References 1 through 4 were generally fine-grained, homogeneous explosives that are apt to behave somewhat differently from a more heterogeneous explosive such as ANFO. Finally, it is possible that the data obtained from the large-scale tests did not represent steady-state values and that for larger charge sizes (longer distances of propagation) higher detonation velocities would be

53

found. The irregularity in the measured detonation trajectories
(presumably caused by incomplete mixing within the bags) makes it
impossible to be absolutely certain that a constant velocity has
been achieved. However, in developing a model for the detonation
properties we will assume that steady-state has been reached and
that the data from the tests is a better representation of the
steady-state behavior of ANFO than the empirical predictions.

4.3 A DETONATION MODEL FOR ANFO

From the test data a mathematical model for the detonation
properties of diluted ANFO was developed. A density of 0.75
gm/cm^3 was selected for use in the MINE THROW II Event. Data from
the large-scale tests indicate that this should have a detonation
velocity of 0.47 cm/μsec. A polytropic gas (constant γ) descrip-
tion of the behavior of the detonation products was used since
no data exist to justify a more complicated model. The variables
at the Chapman-Jouguet state for this explosive (calculated from
Equations 10 through 14) are given in Table 1.

A series of one-dimensional (planar) finite-difference
calculations was performed to determine which rate model gave
the best fit to the measured detonation trajectories. The grain-
burning model with the parameters given in Table 1 gave best
agreement. A comparison between calculated and measured detona-
tion trajectories is shown in Figure 27. The agreement is
reasonably good, although with small changes in the model
parameters a better fit could probably be achieved.

54
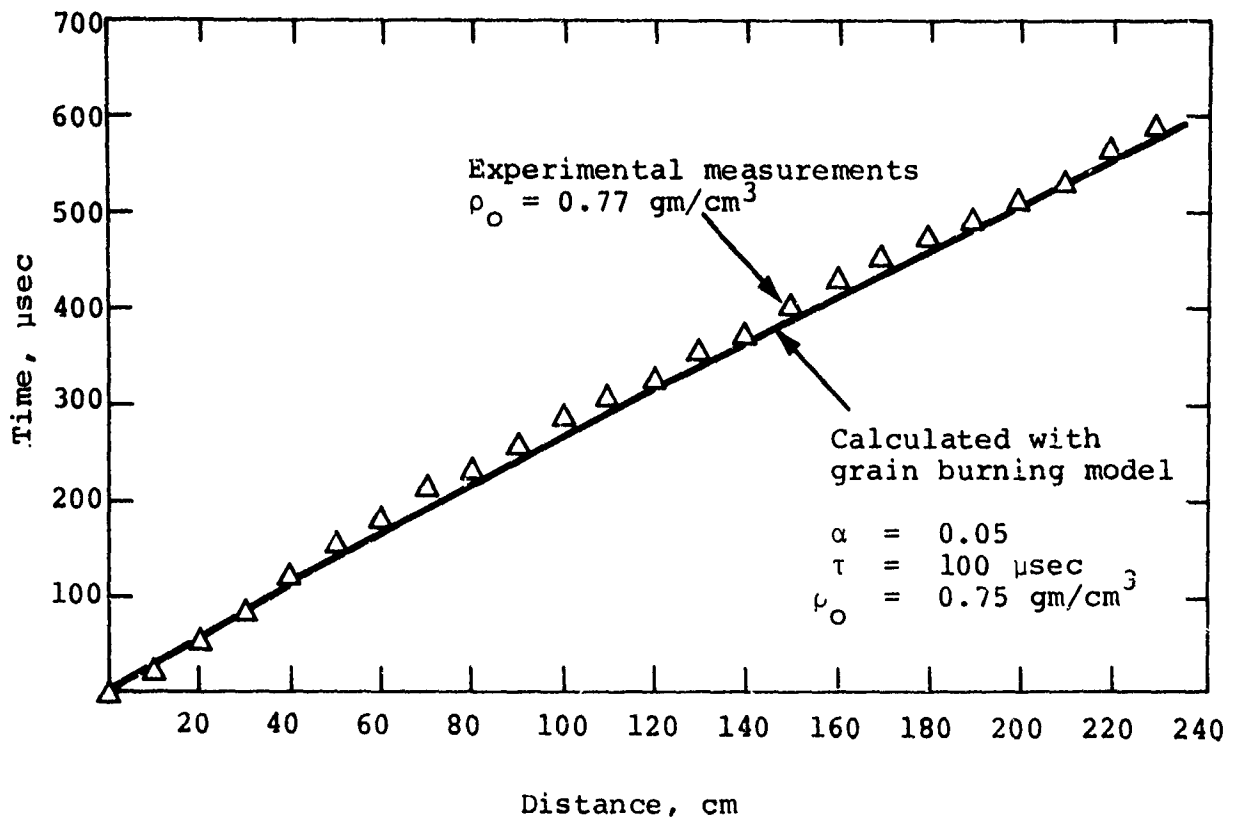
Figure 27   Comparison of measured and calculated detonation
             trajectories for diluted ANFO.

55

TABLE 1

MODEL PARAMETERS FOR DILUTED ANFO

$$\rho_o = 0.75 \text{ gm/cm}^3$$

$$D = 0.47 \text{ cm/}\mu\text{sec}$$

$$Q = 912.8 \text{ cal/gm} = 0.03821 \text{ Mbar-cm}^3\text{/gm}$$

Chapman-Jouguet State Variables	Reaction Rate Model Parameters (Grain-Burning Model)
$P_{CJ} = 0.0558$ Mbar	$\alpha = 0.05$
$\gamma_{CJ} = 1.97$	$\tau = 100$ μsec
$u_{CJ} = 0.158$ cm/μsec	
$v_{CJ}/v_o = 0.312$	

Although this model gives good agreement with the data, this does not mean that it necessarily represents a physically correct model of the ANFO detonation process. Other models for the reaction process and for the equation of state of the reaction products may be more physically realistic. However, the objective of this program was to find a simple model that could adequately describe the ANFO detonation properties in finite difference calculations of the MINE THROW II simulation charge design. Further modeling work is beyond the scope of this program but is recommended for future study.

SECTION 5

SUMMARY AND CONCLUSIONS

The test series discussed in Section 2 demonstrated the feasibility of producing a low-detonation-velocity ANFO explosive by diluting normal-density ANFO with a low-density inert material. Polystyrene beads were found to be the best diluent from the point of view of minimizing both cost and mass of inert material added to the explosive. Although the beads tend to segregate from the ANFO, by mixing the correct proportions of beads and ANFO in each bag, the scale of the density variations can be minimized. Some irregularities in the detonation trajectories of the low-density mixtures were observed which were apparently caused by incomplete mixing within the bags. To prevent possible problems, a better mixing procedure should be developed for the explosive produced for MINE THROW II.

A mixture having a density of 0.75 gm/cm^3 was selected for MINE THROW II. The detonation pressure of this explosive is predicted to be on the order of 56 kilobars, which satisfies the design requirements for the simulation charge. Furthermore, less than 1 percent by mass of the polystyrene diluent is required to achieve this density; this minimizes any effect the diluent may have on the detonation reaction or on the behavior of the reaction products.

A mathematical model of the detonation properties of the low-density ANFO was developed. A Chapman-Jouguet detonation was assumed and a grain-burning reaction rate model (Reference 8) was used to model the reaction process. The data indicated that a distance of propagation of 100 to 150 cm was required to establish a steady-state detonation which, for the reaction rate model used, corresponds to a reaction time of 100 μsec. The detonation parameters of the explosive to be used for the MINE THROW II Event are presented in Table 1.

REFERENCES

1. Mortimer J. Kamlet and S. J. Jacobs, "Chemistry of Detonations, Part I, A Simple Method for Calculating Detonation Properties of C-H-N-O Explosives," J. Chem. Phys., 48, 1 (January 1968).

2. Mortimer J. Kamlet and J. E. Ablard, "Chemistry of Detonations, Part II, Buffered Equilibria," J. Chem. Phys., 48, 1 (January 1968).

3. Mortimer J. Kamlet and Charles Dickenson, "Chemistry of Detonations, Part III, Evaluation of the Simplified Calculational Method for Chapman-Jouguet Detonation Pressures on the Basis of Available Experimental Information," J. Chem. Phys., 48, 1 (January 1968).

4. Mortimer J. Kamlet and Harold Hurwitz, "Chemistry of Detonations, Part IV, Evaluation of a Simple Predictional Method for Detonation Velocities of C-H-N-O Explosives," J. Chem. Phys., 48, 8 (April 1968).

5. F. A. Baum et al., Physics of an Explosion, translated from Fizmatgiz, Moscow (1959) for U.S. Army Engineer Research and Development Laboratories, Fort Belvoir, Virginia, AD 400-151.

6. L. D. Landau and E. M. Lifshitz, Fluid Mechanics, Pergamon Press, Addison-Wesley Publishing Company, Inc., Reading, Massachusetts (1966).

7. Forman A. Williams, Combustion Theory, Addison-Wesley Publishing Company, Inc., Reading, Massachusetts (1965).

8. H. Eyring et al., "The Stability of Detonation," Chem. Rev., 45, 144, (1949) p. 69.

REFERENCES   (cont.)

9. M. Finger, private communication.

10. Melvin A. Cook, The Science of High Explosives, p. 127,
    Reinhold Publishing Corporation, New York (1958).

11. William C. Maurer, Detonation of Ammonium Nitrate in Small
    Drill Holes, Ph.D. Thesis, Colorado School of Mines,
    Golden, Colorado (1961).

12. Fourth Annual Symposium on Mining Research, George B. Clark,
    ed., Bulletin, University of Missouri School of Mines and
    Metallurgy, Rolla, Missouri, Technical Series No. 97 (1959).

13. Fifth Annual Symposium on Mining Research, George B. Clark,
    ed., Bulletin, University of Missouri School of Mines and
    Metallurgy, Rolla, Missouri, Technical Series No. 98 (1960).

14. J. J. Yancik, Monsanto Blasting Products ANFO Manual,
    Monsanto Company, St. Louis, Missouri (May 1969).

15. L. D. Sadwin and J. F. Pittman, Airblast Characteristics of
    AN/FO, Phase I, NOLTR 69-82, U. S. Naval Ordnance
    Laboratory, White Oak, Silver Spring, Maryland (April 1969).

16. L. D. Sadwin and M. M. Swisdak, Jr., Blast Characteristics
    of 20 and 100 Ton Hemispherical AN/FO Charges, NOL Data
    Report, NOLTR-70-32, U. S. Naval Ordnance Laboratory,
    White Oak, Maryland (March 1970).

17. F. M. Sauer, Execution of the MINE THROW I Event, PIFR-374,
    Physics International Company, San Leandro, California,
    to be published.

18. M. Finger, private communication.